Development of Fluorophore-tagged Biodegradable Star Polymers

A Thesis

submitted to

Indian Institute of Science Education and Research Pune in partial fulfilment of the requirements for the BS-MS Dual Degree Programme

by

Vaishak Bhat

20191018

Indian Institute of Science Education and Research Pune

Dr. Homi Bhabha Road,

Pashan, Pune 411008, INDIA.

April, 2024

Supervisor: **Prof M Jayakannan**

Department of Chemistry

Certificate

This is to certify that this dissertation entitled "**Development of Fluorophore-tagged Biodegradable Star Polymers**" towards the partial fulfilment of the BS-MS dual degree programme at the Indian Institute of Science Education and Research, Pune represents study/work carried out by **Vaishak Bhat** at Indian Institute of Science Education and Research, Pune under the supervision of **Prof. M. Jayakannan**, Department of Chemistry, during the academic year 2023-2024.

Prof. M. Jayakannan
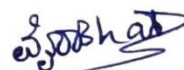
Date: 20/05/2024

Place: IISER Pune

Committee:

Prof. M. Jayakannan

Dr. J. Nithyanandhan

Declaration

I hereby declare that the matter embodied in the report entitled "**Development of Fluorophore-tagged Biodegradable Star Polymers**" are the results of the work carried out by me at the Department of Chemistry, Indian Institute of Science Education & Research (IISER) Pune, under the supervision of **Prof. M Jayakannan**, and the same has not been submitted elsewhere for any other degree. Wherever others contribute, every effort is made to indicate this clearly, with due reference to the literature and acknowledgment of collaborative research and discussions.

Vaishak Bhat

20191018

20|05|2024

Acknowledgments

I want to express my sincere gratitude to my supervisor, Prof. M Jayakannan, for giving me this opportunity to learn and explore the field of polymer chemistry and for his constant enthusiasm and support for the practice of science.

I thank Dr. J Nithyanandhan, who has been my TAC member and provided valuable guidance in shaping my project.

I thank my mentor, Pathan Shahidkhan, for teaching me the skills and techniques I needed for the project and guiding me when I was uncertain.

I thank Ashutosh, Rhujal, and Sanchi for always being there for me whenever I needed help. I thank Parshuram, Utreshwar, Khuddus, Mishika, Akshay, Sunidhi, Bhushan, and Pooja for their constant support and for making my time in the lab pleasant.

I am grateful to my previous mentors, Rahul, Manjeet, and Sachin, for teaching me the basic skills of organic synthesis and work management in lab.

I want to thank all my friends, without whom my time here at IISER wouldn't have been so smooth. I am indebted to the IISER Pune community- professors, non-teaching staff, classmates, juniors, and seniors. This community has truly been my second family for the past five years.

I am thankful to the technical staff in the chemistry department because of whom the project was able to progress steadily.

I would like to acknowledge the KVPY program for financial support.

Finally, I give my heartfelt gratitude to my family, because of whom all this has been possible.

Table of Contents

List of figures

Abbreviations

AIE – Aggregation induced emission

AIEgen – Molecule exhibiting AIE attributes

DCM – Dichloromethane

DLC – Drug loading content

DLE – Drug loading efficiency

DLS – Dynamic light scattering

DMF – Dimethylformamide

DSC – Differential scanning calorimetry

EA – Ethyl acetate

ε-BCL – Boc-substituted ε-caprolactone

f_w – Fraction of water (used here in terms of percentage)

MTT – 4,5-Dimethylthiazol-2-yl)-2,5-diphenyltetrazolium bromide

PBS – Phosphate buffered saline

PCC – Pyridinium chlorochromate

RB – Round bottom flask

SEC – Size exclusion chromatography

THF – Tetrahydrofuran

TGA – Thermogravimetric analysis

T_g – Glass transition temperature

TPE – Tetraphenyl ethylene

Abstract

This work showcases the design of a novel TPE (tetraphenyl ethene)-based initiator library with initiating sites varying from two to eight. The synthesized hydroxy-functionalized TPE derivatives could be utilized for the ROP (ring-opening polymerization) of a tailor-made carboxy-substituted caprolactone using tin-based catalyst $Sn(Oct)_2$ in melt conditions. The polymers thus synthesized are biodegradable due to the aliphatic ester backbone and fluorescent due to the AIE (aggregation induced emission) activity of TPE. NMR, SEC, and thermal characterizations of the polymers were carried out. Deprotection of the Boc group resulted in amphiphilic polymers, which were self-assembled and monitored for their photophysical properties. The studies reveal that the fluorescence intensity of the resulting star polymers is dependent on the substitution of the TPE core- the higher the substitution at the core, the higher the fluorescence intensity due to AIE. The polymers are amenable to bioimaging due to the presence of TPE. This was confirmed by cellular uptake studies which showed localization of polymer in the cytoplasm. The polymers were also found to be non-toxic to cells. Anticancer drug encapsulation studies revealed that they can load DOX with a DLC of ~2%. These drug-loaded polymers were found to be as effective as free DOX in cytotoxicity. The synthesized TPE-PCL system thus shows promising theranostic applications, along with providing an opportunity to study TPE photophysics.

1. Introduction

1.1. Polymers and drug delivery:

The creation of specific, efficient, and non-toxic drugs for disease treatment has been a longstanding quest in the field of medicine. With the rapid advancement of science and technology in the recent century, we are inching closer every day towards solving this quest. The knowledge of organic chemistry made the jump from naturally available drugs to artificially synthesizable drugs possible. Yet, direct intake of free drugs has some issues: small therapeutic window, non-specific targeting (leading to damage of healthy cells and tissues), solubility (in the case of hydrophobic molecules), biodistribution and bioavailability. These problems can be overcome with the use of drug delivery vehicles or nanocarriers[1]. Cancer, the disease caused by the abnormal proliferation of cells in the body, is the second leading cause of death globally. Nanocarrier-based drug delivery has been one of the successful approaches to combat cancer[2–4].

The following factors become essential to build an effective nanocarrier system for cancer treatment: 1) Circulation in blood; 2) Accumulation at the tumor site; 3) Penetration through tumor mass; 4) Internalization of the carrier into the cancer cells; and 5) Release of the loaded cargo[5]. Proper blood circulation calls for the nanocarrier to be water-soluble, non-immunogenic and not have a high renal clearance. Another critical aspect is that the nanocarrier should be selectively able to target the tumor cells and not the healthy cells. This is achieved by making use of the EPR (Enhanced Permeability and Retention) effect[6]. Tumor tissues are distinct from healthy tissues in that they have a leaky vasculature (which is helpful in tumor progression), i.e., large irregular intercellular spaces. Healthy tissues have a tight vasculature. When the nanoparticles are 20-200 nm in size, they can pass through the tumor tissue but not the healthy tissues. Additionally, the tumor tissues have a defective lymphatic drainage system, thus increasing nanocarrier availability at the tumor site[7]. Along with this tissue-level identification, the nanoparticle must be able to internalize into the cancer cells and release the loaded drug upon some specific intracellular trigger.
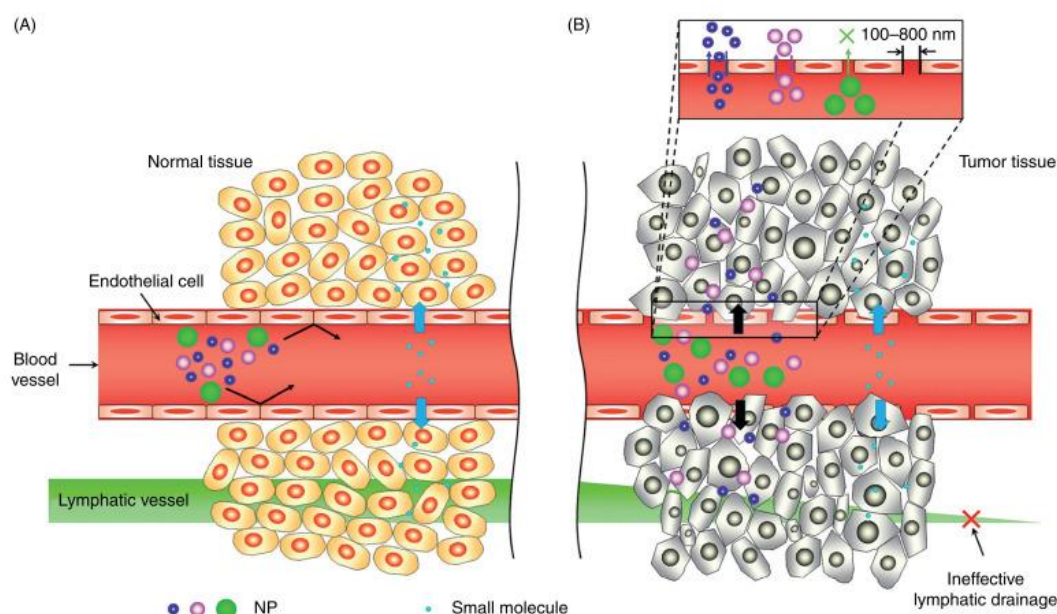
Figure 1: Demonstrating the EPR effect

Differential uptake of nanoparticles of different sizes in (A) Normal tissue and (B) Tumor tissue (Reprinted from reference[8])

Polymer-based drug delivery can be categorized into polymeric drugs, polymer-drug conjugates, polymer–protein conjugates, polyplexes and polymeric micelles[9]. Polymers which are amphiphilic, i.e. having distinct hydrophobic and hydrophilic blocks, undergo phase segregation in water, where the hydrophobic parts of the polymer come together and get buried away from the aqueous phase while the hydrophilic parts interact with water. This thermodynamically favored process results in the formation of nanoparticles that can have a variety of structures, such as vesicles, spherical micelles, and cylindrical micelles[10]. The ability to incorporate and load high content of both hydrophobic and hydrophilic drugs, ease of growing polymers (especially with the recent development of controlled radical polymerizations), variety of architectures (linear, hyperbranched, dendritic, bottlebrush, star, etc.) as well as the possibility of incorporating innumerable combinations of functional handles make the research in the field of polymeric nanocarriers a rich one[11].
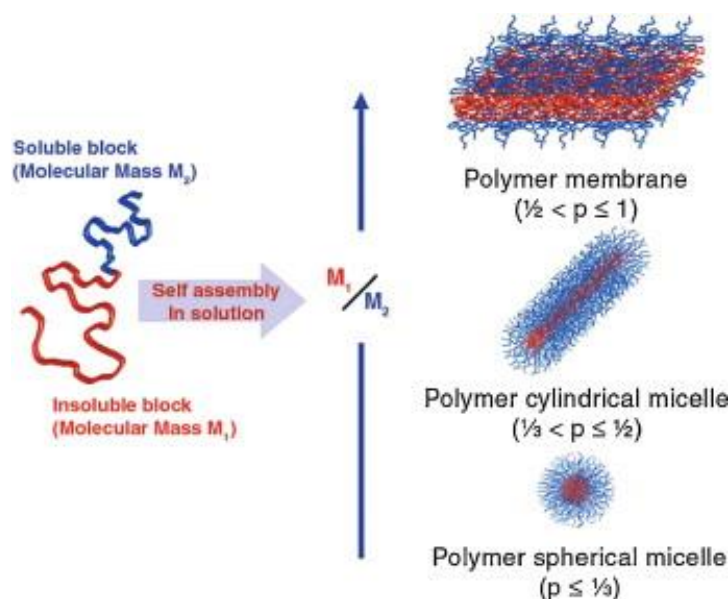
Figure 2: Self-assembly of an amphiphilic block copolymer

Different architectures that can form from a block copolymer. p refers to the critical packing parameter, which indicates the geometry adopted by the polymer. (Reprinted from reference[12])

1.2. Biodegradable polymers:

Complete clearance of nanoparticles from the body is not assured, and hence, biodegradability is a preferred feature for a nanoparticle system for drug delivery. Such nanocarriers also tend to be non-toxic, biocompatible, and non-immunogenic, making them ideal candidates for our purpose[13]. One class of polymers that fall into this category are aliphatic polyesters. These polymers are enzymatically degradable in the body. Examples of polyesters include polyglycolic acids, polylactides, and polycaprolactones, among others. Polycaprolactone (PCL) is a fossil-fuel-based polyester that is soluble in many common organic solvents such as toluene, chloroform, and dichloromethane as well as miscible with many polymers like PVC and polycarbonates[14]. PCL has found enormous applications in the creation of blends, composites, and scaffolds for tissue engineering. Also, PCL is advantageous over other aliphatic esters because of the possibility of functionalizing them[15], which opens up opportunities such as modulating hydrophobicity, conjugating drugs, inducing stimuli responsiveness, etc. There are two known methods of PCL polymerization – condensation of 6-hydroxyhexanoic acid and ROP (Ring Opening Polymerization) of

ε-caprolactone. ROP involves the ring opening of the seven-membered ring, where the relieving of torsional strain is the driving force for polymerization. This is the preferred method due to the higher quality of polymers generated – polycondensation route gives highly disperse polymer wherein achieving high molecular weight is difficult. In contrast, the ROP route gives narrow disperse polymers with high molecular weight. There are primarily four mechanisms for the ROP of lactones – cationic, anionic, monomer-activated, and coordination-insertion.

Coordination-insertion ROP is a pseudo-anionic polymerization where the monomer gets inserted into a metal-oxygen bond following coordination with the metal catalyst. Of the known catalysts for this mechanism, the tin-based catalyst stannous octoate (Sn(Oct)$_2$) is the most popular as it is highly effective, commercially available, easy to handle, and soluble in common organic solvents. One of the disadvantages of this system is the high reaction temperature, which increases the chances of transesterification[14].
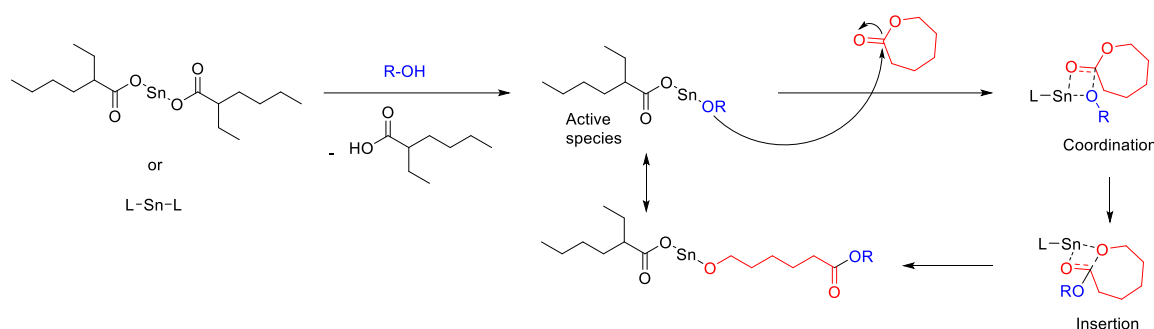
Figure 3: Coordination-insertion ROP mechanism of the Sn(Oct)2 catalyst

1.3. Star polymers:

Star polymers are spatially defined polymers with a core-shell-periphery type of arrangement, yet having a compact 3-dimensional structure[16]. They are an attractive class of single polymer nanocarriers with the advantage of one-pot synthesis and narrow dispersity of the polymers. Star polymer synthesis can be undertaken in three ways – core-first, arm-first, and grafting-onto. While each method has its advantages and shortcomings, in the core-first approach, it is easy to separate pure polymers from the monomer, catalyst, and other impurities by precipitation, with excellent yields. This approach involves growing polymer from a functional core with multiple initiating sites

with equal reactivity. Previous work from our group[17] has shown that star polymers with higher number of arms (>4) can form unimolecular micelles. Unimolecular micelles are a next-generation micellar system where each star-polymer molecule collapses upon itself in the aqueous medium to form a micelle. Thus, the concept of critical micelle concentration becomes void, where a threshold concentration of molecules is necessary to form a micelle. Unimolecular micelles are unaffected by dilution, which is one of the destabilizing factors for a nanocarrier medication once it enters the body.
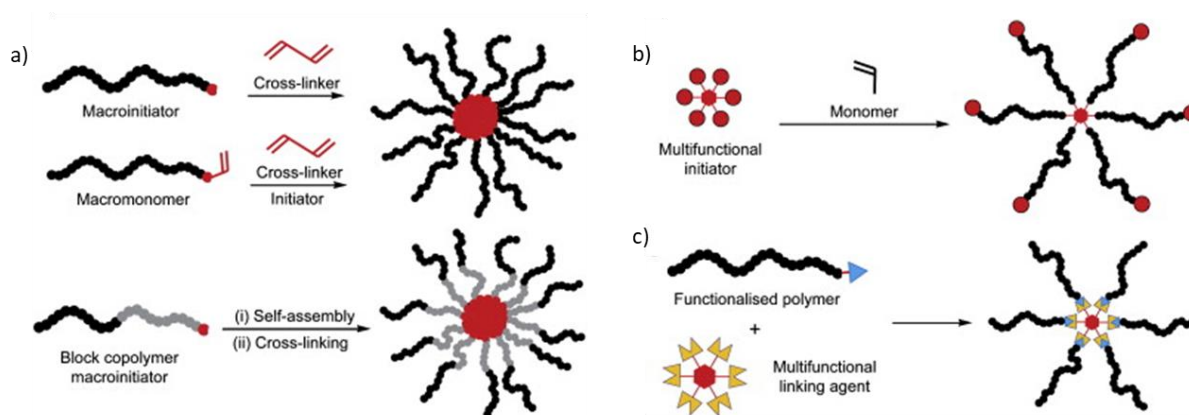
Figure 4: Strategies for star polymer synthesis

a) Arm-first; b) Core-first; and c) Grafting-onto approaches for star polymer synthesis (adapted from reference[18])

1.4. Fluorescent polymers:

For any new nanoparticle system that we create, a crucial aspect is to track the system's fate inside the cells, such as location, degradation, and clearance with time. Some conventional methods include using fluorescent drugs to indirectly track the fate of the polymer by monitoring the drug's fluorescence or incorporating conventional chromophores by covalent binding to the polymer. Most commonly used fluorophores undergo quenching in aggregated state, leading to damping of fluorescence. This phenomenon, called aggregation-caused quenching (ACQ), has limited the synthesis of fluorescent polymers. But there is another class of fluorophores, in which they are non-fluorescent when soluble in a particular solvent but fluorescent in the aggregated state (i.e., when they are insoluble in some solvent). This phenomenon has been termed as aggregation-induced emission (AIE)[19]. AIE polymers have gained

considerable interest not just in the biomedical area but also in optoelectronics and sensing applications. Tetraphenyl ethene (TPE) is a well-known AIE molecule. In the solution state, the excited molecule loses energy non-radiatively, primarily by the phenyl ring rotation at the ethene-phenyl single bonds. In the aggregated state, the intermolecular steric hindrance restricts this rotation. This is termed as restriction of intramolecular motion (RIM). Now with the non-radiative path blocked, the excited molecule returns to the ground state radiatively, leading to fluorescence.
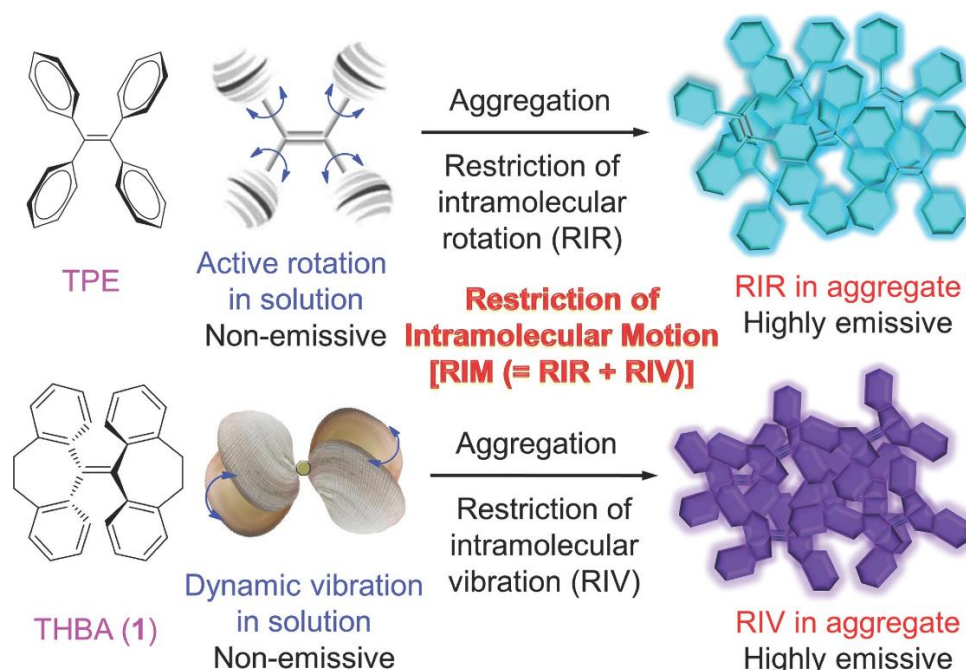
Figure 5: AIE arising from RIM

Activation of AIE in the solid state for TPE through restriction of intramolecular rotation (RIR) (above) and for THBA through restriction of intramolecular vibration (RIV) (below). In a single molecular species, RIR and RIV can go hand-in-hand to bring about RIM (Figure reprinted from reference[20])

1.5. Biodegradable fluorescent star-polymers:

Incorporating AIE molecules into star polymers can be achieved in one of four ways: a) Polymerization of AIEgen-containing monomer; b) Polymerization from AIEgen-containing initiators; c) Post-polymerization modification with AIEgens; d) In-situ AIEgen formation from non-AIE-active precursors[21]. This work aims at creating a fluorescent star-polymer system using functionalized TPE as the initiator. The number of initiating sites will be varied to create a series of polymers with arm numbers from

2 to 8. Along with playing the initiator role, TPE will also act as the hydrophobic core of our system. A carboxy-substituted caprolactone, t-butyl-3-((7-oxooxepan-4-yl)oxy)-propanoate will be used for the hydrophilic shell. This monomer has proven to be efficacious in drug delivery applications due to its drug loading ability and pH responsiveness[22,23].

The use of this TPE-PCL system is threefold- 1) The influence of the 3D polymer architecture on the AIE property of TPE can be systematically studied; 2) All the synthesized polymers will be fluorescent, with the AIE of TPE achieved by RIM of the phenyl rings due to the bulky polymer chains around it. The fate of the polymeric micelles inside the cells can thus now be directly tracked; 3) TPE forms a FRET pair with many well-known drugs and dyes such as doxorubicin and nile red. The FRET process can be utilized to monitor the drug release kinetics of the micelles.

AIE phenomenon has already found extensive bioimaging applications[24]. Our group has utilized TPE-based polymers for applications such as drug delivery and antimicrobial activity using different design strategies - by conjugating TPE molecules to the polymer backbone[25] or by synthesizing TPE-initiated polymers[26].

Structure-property relationship (SPR) studies on TPE have been carried out by Wei and coworkers[21], where they have followed the emission properties of TPE-initiated polymers having 2, 3, and 4 arms. This work aims to lay the groundwork for a more extensive, systematic study of TPE photophysics using polymer chemistry as a tool and enhance our current understanding of the topic.

2. Materials and methods

2.1. Materials:

Benzophenone, boron tribromide, 3-chloroperbenzoic acid, 1,6-cyclhexanediol, 4,4'-dihydroxybenzophenone, doxorubicin hydrochloride, ethanolamine, ethyl chloroacetate, 4-hydroxybenzophenone, methyl iodide, potassium tert-butoxide, pyridinium chlorochromate, serinol, tert-butyl acrylate, tin(II) 2-ethylhexanoate, titanium tetrachloride, trifluoroacetic acid, and trizma base were purchased from Sigma Aldrich. NaCl, Na_2SO_4, K_2CO_3, $NaHCO_3$, and HCl were purchased locally. The solvents used were DCM, methanol, ethyl acetate, diethyl ether, hexane, DMF, and THF.

2.2. Instrumentation:

^{1}H-NMR and ^{13}C-NMR were recorded using 400MHz Bruker spectrophotometer. SEC of the polymer samples was performed with chloroform as eluent and polystyrene as standard for calibration using Viscotek VE 3580 RI, 3210 UV-Vis and light scattering detectors and Viscotek VE 1122 pump. For the thermal characterization of the initiators and polymers, Perkin-Elmer thermal analyzer STA 6000 was used for TGA analysis with a heating rate of 10°C/min from 30°C to 600°C. TA Q20 instrument was used for DSC analysis, where the samples were subject to heating and cooling cycles at the rate of 10°C/min under constant nitrogen supply. Photophysical studies were carried out using a Perkin-Elmer Lambda 45 UV-Visible Spectrophotometer for absorption and a SPEX Fluorolog HORIBA fluorescence spectrophotometer with a 150W Xe lamp for fluorescence measurements. DLS measurements were performed using a Nano ZS-90 Malvern instrument with a 633 nm laser, with detection at 90° angle light scattering. Absorbance measurement for the MTT assay was performed using the Varioskan plate reader. The cellular uptake of polymers was visualized using a Leica SP8 confocal microscope.

2.3. Synthesis:

2.3.1. Synthesis of the initiators:

2.3.1.1. Synthesis of TPE-1-OH and TPE-2-OH:

The McMurry reaction for TPE synthesis was performed in the following manner: Benzophenone (8.82g, 48.4 mmol), 4-Hydroxybenzophenone (8g, 40.4 mmol), and Zn dust (11.6g, 177.6 mmol) were weighed in an RB. The RB was kept in an ice bath after transferring dry THF (250 mL). $TiCl_4$ (9.74 mL, 88.8 mmol) was transferred using a cannula. The ice bath was removed, and the system was allowed to come to room temperature. The setup was then kept for reflux at 70°C for 12 hours. This reaction results in the self and cross-products between the reactants, yielding TPE, TPE-1-OH, and TPE-2-OH. After determining reaction completion by TLC, RB was kept in an ice bath, and HCl (1N, 300 mL) was added. The reaction mixture was then extracted with DCM (150 mL). DCM was washed with brine and passed through anhydrous Na_2SO_4. DCM was evaporated and column chromatography was performed to isolate TPE-1-OH and TPE-2-OH. TPE-1-OH: ^{1}H NMR (400 MHz, $CDCl_3$) δ 7.15 – 6.98 (m, 15H), 6.91 – 6.87 (m, 2H), 6.59 – 6.54 (m, 2H); TPE-2-OH: ^{1}H NMR (400 MHz, DMSO) δ 9.30 (d, J = 11.3 Hz, 2H), 7.16 – 7.02 (m, 6H), 6.98 – 6.90 (m, 4H), 6.77 – 6.67 (m, 4H), 6.54 – 6.45 (m, 4H)

2.3.1.2. Synthesis of 4,4'-dimethoxybenzophenone (MBP):

Firstly, 4,4'-dihydroxybenzophenone (10g, 47 mmol) was weighed in an RB. DMF was added and the reactant was solubilized. K_2CO_3 (25g, 188 mmol) was added to the RB and kept for stirring for 30 minutes. After the reaction mixture turned greenish, it was transferred to an ice bath, and methyl iodide (11.7 mL, 188 mmol) was added dropwise. The ice bath was removed after 15 minutes. TLC was undertaken to determine reaction completion. The reaction mixture was then taken in a separating funnel and washed with chilled water. This mixture was extracted thrice with ethyl acetate. The combined organic fraction was washed twice with chilled water and passed through anhydrous Na_2SO_4. Ethyl acetate was evaporated to yield the product. ^{1}H NMR (400 MHz, $CDCl_3$) δ 7.83 – 7.75 (m, 4H), 7.00 – 6.92 (m, 4H), 3.89 (s, 6H).

2.3.1.3. Synthesis of TPE-4-OMe:

TPE-4-OMe was synthesized by the McMurry coupling of 4,4'-dimethoxybenzophenone (10g, 41 mmol) using Zn dust (6.1g, 93 mmol), TiCl$_4$ (5.1 mL, 41 mmol), and dry THF (150 mL). The reaction was performed as described in TPE-mOH synthesis. After the reaction, the reaction mixture was filtered, concentrated, and precipitated in MeOH. Removal of MeOH followed by drying yielded pale pink colored powder. ^{1}H NMR (400 MHz, CDCl$_3$) δ 6.97 – 6.89 (m, 4H), 6.68 – 6.60 (m, 4H), 3.74 (s, 6H).

2.3.1.4. Synthesis of TPE-4-OH:

TPE-4-OMe (4.4g, 9.7 mmol) was weighed in an RB. Dry DCM (25 mL) was added, and the mixture was kept in a dry ice bath to maintain -78°C. BBr$_3$ (7.3 mL, 77 mmol) was taken in a measuring cylinder. It was made into a 25 mL solution using DCM. This solution was poured carefully into the RB. The reaction mixture turned dark violet from pinkish orange. The dry ice bath was removed after an hour, and the reaction was kept at room temperature for 10 hours. After confirming reaction completion by TLC, RB was kept in an ice bath followed by slow addition of water. After the evolution of fumes had stopped, DCM was removed, and the resulting mixture was extracted twice using diethyl ether. The combined organic layer was washed thrice with water. The mixture was then washed with brine, passed through Na$_2$SO$_4$, and concentrated to get reddish-white product. ^{1}H NMR (400 MHz, DMSO) δ 9.22 (s, 4H), 6.73 – 6.66 (m, 8H), 6.51 – 6.45 (m, 8H).

2.3.1.5. Synthesis of TPE-1-ester:

TPE-1-OH (4g, 11.5 mmol) and anhydrous K$_2$CO$_3$ (4.76g, 34.4 mmol) were weighed in an RB. Dry DMF was transferred to the RB, and after about 90 minutes, ethyl chloroacetate (1.84 mL, 17.2 mmol) was transferred using a syringe. The dark yellow suspension became more greenish. After the reaction, cold water was added to the reaction mixture. The mixture was extracted twice with ethyl acetate. The combined organic layers were washed twice with cold water. The organic layer was dried using anhydrous Na$_2$SO$_4$, concentrated, and purified by column with EA:Hexane (1:25 v/v) to yield a green viscous liquid. DCM was added and left overnight to yield a white compound. ^{1}H NMR (400 MHz, CDCl$_3$) δ 7.09 (dtt, J = 7.7, 4.8, 2.2 Hz, 9H), 7.02 (tdd,

J = 6.7, 5.0, 3.0 Hz, 6H), 6.96 – 6.91 (m, 2H), 6.66 – 6.61 (m, 2H), 4.54 (s, 2H), 4.25 (q, J = 7.1 Hz, 2H), 1.27 (t, J = 7.1 Hz, 3H).

2.3.1.6. Synthesis of TPE-2-ester:

Reaction was performed similar to the TPE-1-ester synthesis using TPE-2-OH (1.5g, 4.1 mmol), anhydrous K_2CO_3 (2.85g, 20.6 mmol), and ethyl chloroacetate (1.1 mL, 10.3 mmol) in dry DMF (15 mL). Workup and column chromatography (1:13 v/v EA:Hexane) were carried out to yield green viscous liquid. ^{1}H NMR (400 MHz, CDCl$_3$) δ 7.13 – 7.05 (m, 6H), 7.00 (ddd, J = 9.6, 5.2, 2.4 Hz, 4H), 6.95 – 6.88 (m, 4H), 6.67 – 6.59 (m, 4H), 4.54 (d, J = 7.1 Hz, 4H), 4.25 (qd, J = 7.1, 5.6 Hz, 4H), 1.28 (td, J = 7.1, 5.7 Hz, 6H).

2.3.1.7. Synthesis of TPE-4-ester:

Reaction was performed similar to the TPE-1-ester synthesis using TPE-4-OH (3.2g, 8.1 mmol), anhydrous K_2CO_3 (11.2g, 80.7 mmol), and ethyl chloroacetate (8.64 mL, 80.7 mmol) in dry DMF (45 mL). Workup and column chromatography (1:4 v/v EA:Hexane) were carried out to yield the desired product. ^{1}H NMR (400 MHz, CDCl$_3$) δ 6.93 – 6.87 (m, 8H), 6.66 – 6.59 (m, 8H), 4.54 (s, 8H), 4.26 (q, J = 7.1 Hz, 8H), 1.28 (t, J = 7.2 Hz, 12H).

2.3.1.8. Synthesis of T2:

TPE-2-ester (400 mg, 0.74 mmol), and ethanolamine (900 μL, 14.88 mmol) were taken in an RB to which MeOH (2 mL) was added. The reaction was stirred for 2 hours, resulting in a white paste-like mixture. MeOH was first evaporated. This was followed by solvent extraction in DCM:Water system. DCM was then evaporated to yield white powder. ^{1}H NMR (400 MHz, DMSO) δ 7.96 (q, J = 6.0 Hz, 2H), 7.19 – 7.04 (m, 6H), 7.00 – 6.91 (m, 4H), 6.91 – 6.82 (m, 4H), 6.78 – 6.69 (m, 4H), 4.70 (td, J = 5.5, 3.6 Hz, 2H), 4.38 (d, J = 8.8 Hz, 4H), 3.41 (qd, J = 6.0, 4.1 Hz, 4H), 3.19 (qd, J = 6.1, 4.1 Hz, 4H); ^{13}C NMR (101 MHz, CDCl$_3$) δ 144.60, 137.11, 135.94, 133.08, 132.97, 119.34, 119.23, 72.01, 64.84, 46.35, 45.36, 45.15, 44.94, 44.73, 44.52, 44.31, 44.10.

2.3.1.9. Synthesis of T3:

TPE-1-ester (200 mg, 0.46 mmol), tris base (575 mg, 4.6 mmol), and MeOH (5 mL) were taken in an RB and kept for reflux at 70°C. MeOH was removed post reaction and the reaction mixture was extracted in EA:Water system. Ethyl acetate was evaporated to yield the desired product. ^{1}H NMR (400 MHz, CDCl$_3$) δ 7.58 (s, 1H), 7.15 – 7.06 (m, 9H), 7.05 – 6.99 (m, 6H), 6.99 – 6.94 (m, 2H), 6.69 – 6.63 (m, 2H), 4.44 (s, 2H), 3.65 (s, 6H).

2.3.1.10. Synthesis of T4:

TPE-4-ester (500 mg, 0.68 mmol), ethanolamine (820 µL, 13.5 mmol), and MeOH (4 mL) were taken and sonicated to disperse the contents. Reaction was kept to stir. A milky white suspension formed from which MeOH was evaporated. DCM was added to the mixture and sonicated. The white compound was only slightly soluble in DCM. The contents were filtered through a Whatman filter paper to yield a white solid.
^{1}H NMR (400 MHz, DMSO) δ 7.96 (t, J = 5.7 Hz, 4H), 6.90 – 6.81 (m, 8H), 6.77 – 6.69 (m, 8H), 4.70 (s, 4H), 4.38 (s, 8H), 3.45 – 3.39 (m, 9H), 3.19 (q, J = 6.1 Hz, 8H).
^{13}C NMR (101 MHz, DMSO) δ 168.02, 156.40, 138.65, 137.21, 132.41, 114.52, 67.26, 60.09, 44.04, 41.60.

2.3.1.11. Synthesis of T6:

TPE-2-ester (320 mg, 0.6 mmol), tris base (720 mg, 5.94 mmol), and MeOH (5 mL) were taken in an RB and kept for reflux at 70°C. After reaction completion, MeOH was evaporated and solvent extraction was done in EA:Water system. Ethyl acetate was evaporated to yield the desired product. ^{1}H NMR (400 MHz, DMSO) δ 7.19 – 7.06 (m, 8H), 6.99 – 6.93 (m, 4H), 6.91 – 6.83 (m, 4H), 6.79 – 6.69 (m, 4H), 4.76 (td, J = 5.7, 3.2 Hz, 6H), 4.38 (d, J = 8.1 Hz, 4H), 3.57 (dd, J = 5.7, 4.2 Hz, 12H).
^{13}C NMR (101 MHz, DMSO) δ 168.29, 156.26, 156.22, 144.02, 139.86, 136.93, 132.43, 131.19, 128.35, 128.23, 126.92, 126.85, 114.68, 114.57, 67.40, 62.30, 60.44.

2.3.1.12. Synthesis of T8:

TPE-4-ester (500 mg, 0.68 mmol), serinol (1230 mg, 13.5 mmol), and MeOH (5 mL) were taken in an RB and kept to stir at room temperature. The turbidity of the reaction mixture increased through the course of the reaction. MeOH was evaporated. The

contents were redispersed in MeOH and filtered through Whatman paper to yield a reddish-white crispy solid. ^{1}H NMR (400 MHz, DMSO) δ 7.55 (d, J = 8.4 Hz, 4H), 6.90 – 6.82 (m, 8H), 6.78 – 6.69 (m, 8H), 4.70 (t, J = 5.5 Hz, 8H), 4.41 (s, 8H), 3.83 – 3.74 (m, 4H), 3.49 – 3.38 (m, 17H).

^{13}C NMR (101 MHz, DMSO) δ 167.76, 156.38, 138.62, 137.20, 132.43, 114.53, 67.23, 60.36, 53.00.

2.3.2. Synthesis of the Boc-caprolactone monomer:

2.3.2.1. Synthesis of tert-butyl 3-((4-hydroxycyclohexyl)oxy)propanoate:

1,4-cyclohexanediol (35g, 0.301 mol) was weighed in an RB. Dry THF (400 mL) was transferred to the RB. A catalytic amount of potassium tert-butoxide was added, and this setup was kept at 40°C for 30 minutes. Tert-butyl acrylate (35.3 mL, 0.241 mol) was dissolved in 60 mL dry THF and added dropwise to the above reaction mixture at room temperature. The reaction was kept in a nitrogen environment and kept for reflux for 24 hours. After the reaction, THF was evaporated and DCM was added. Unreacted diol precipitated, which was filtered, and the filtrate was concentrated to get crude product. Column chromatography was carried out in EA:Hexane (1:10 v/v) to obtain the pure product. Yield – 17.3g (24%).

^{1}H NMR (400 MHz, CDCl$_3$) δ 3.66 (dt, J = 10.8, 6.5 Hz, 3H), 3.33 (dtt, J = 43.4, 6.2, 3.5 Hz, 1H), 2.46 (td, J = 6.4, 5.1 Hz, 2H), 2.04 – 1.89 (m, 2H), 1.81 (ddd, J = 12.7, 10.3, 5.6 Hz, 1H), 1.71 – 1.59 (m, 3H), 1.45 (d, J = 2.8 Hz, 9H), 1.35 – 1.27 (m, 2H).

^{13}C NMR (101 MHz, CDCl$_3$) δ 171.25, 171.14, 80.49, 80.47, 76.84, 74.19, 69.64, 68.52, 64.04, 63.64, 36.80, 36.78, 32.62, 30.45, 29.22, 28.13, 28.11, 27.54.

2.3.2.2. Synthesis of tert-butyl 3-((4-oxocyclohexyl)oxy)propanoate:

Freshly dried molecular sieves were taken in an empty RB. Tert-butyl 3-((4-hydroxycyclohexyl)oxy)propanoate (17.3g, 71 mmol) was taken along with dry DCM (350 mL). PCC (30.6g, 141 mmol) was added, and the reaction was stirred for 8 hours. The reaction mixture was filtered and concentrated. The crude product was taken for column purification in EA:Hexane system (1:20 v/v) to get the yellowish product. Yield – 16.1g (94%).

^{1}H NMR (400 MHz, CDCl$_3$) δ 3.77 – 3.68 (m, 3H), 2.57 (ddd, J = 15.7, 10.8, 5.8 Hz, 2H), 2.50 (t, J = 6.2 Hz, 2H), 2.28 – 2.19 (m, 2H), 2.14 – 2.05 (m, 2H), 1.90 (dddd, J = 14.8, 13.4, 5.1, 2.9 Hz, 2H), 1.45 (s, 9H).

^{13}C NMR (101 MHz, CDCl$_3$) δ 211.50, 171.06, 80.65, 72.84, 64.10, 37.08, 36.64, 30.48, 28.11.

2.3.2.3. Synthesis of tert-butyl 3-((7-oxooxepan-4-yl)oxy)propanoate:

To an RB containing tert-butyl 3-((4-oxocyclohexyl)oxy)propanoate (10g, 41.3 mmol) in DCM (250 mL), mCPBA (14.2g, 82.6 mmol) and NaHCO$_3$ (10.4g, 124 mmol) were added. The reaction was stirred for 20 hours. The solid mass was removed by filtration. The filtrate was treated twice with saturated NaHCO$_3$ solution. The organic layer was passed through anhydrous Na$_2$SO$_4$ and concentrated. The crude product was purified by column chromatography in EA:Hexane (1:10 v/v) to obtain the desired substituted caprolactone monomer. Yield – 8.12g (76%).

^{1}H NMR (400 MHz, CDCl$_3$) δ 4.51 – 4.42 (m, 1H), 4.04 (ddd, J = 13.0, 6.1, 1.8 Hz, 1H), 3.72 – 3.61 (m, 3H), 2.96 (ddd, J = 14.1, 12.1, 1.7 Hz, 1H), 2.47 (dd, J = 6.4, 5.7 Hz, 2H), 2.40 (ddd, J = 14.2, 8.2, 1.5 Hz, 1H), 2.09 – 1.96 (m, 2H), 1.96 – 1.87 (m, 1H), 1.85 – 1.75 (m, 1H), 1.45 (s, 9H).

^{13}C NMR (101 MHz, CDCl$_3$) δ 176.17, 170.92, 80.73, 73.96, 63.96, 63.33, 36.49, 33.88, 28.12, 27.79, 27.33.

2.3.3. Synthesis of the TPE-BPCL homopolymers:

General procedure: The required TPE initiator (1 eq) is taken in a Schlenk polymerization tube. We are aiming for ten monomer units per arm. Hence, [10*number of arms of initiator] equivalents of Boc-caprolactone are transferred to the tube. Sn(Oct)$_2$ (0.5 eq) is then added, followed by keeping the tube under high vacuum for about 45 minutes. Then the tube is immersed in an oil bath at 130°C, and the reaction is kept to stir for an amount of time depending on the arm number (For the synthesis of polymers having arm number 4 and above, overhead mechanical stirring is employed as magnetic stirring doesn't work due to significant viscosity buildup). After the polymerization, the reaction mixture is dissolved in 1-2 mL THF and precipitated in 70 mL cold Et$_2$O:Hexane (4:3 v/v). This setup is kept at 0°C for a few hours before decantation and drying.

2.3.3.1. Synthesis of T2B:

ε-BCL (400 mg, 1.55 mmol), T2 (44 mg, 0.078 mmol), and $Sn(Oct)_2$ (13 μL, 0.04 mmol) were taken in a Schlenk tube and subjected to polymerization for 4 hours. Yield – 180 mg (41%).

^1H NMR (400 MHz, $CDCl_3$) δ 7.14 – 7.04 (m, 6H), 7.04 – 6.90 (m, 10H), 6.70 – 6.61 (m, 4H), 4.42 (d, J = 8.3 Hz, 4H), 4.21 – 4.06 (m, 36H), 3.77 – 3.56 (m, 42H), 3.48 – 3.39 (m, 16H), 2.43 (t, J = 6.3 Hz, 34H), 2.40 – 2.31 (m, 35H), 1.95 – 1.64 (m, 106H), 1.44 (s, 146H).

^{13}C NMR (101 MHz, $CDCl_3$) δ 173.50, 170.87, 132.75, 131.27, 80.59, 75.46, 64.80, 61.25, 36.48, 32.92, 29.69, 28.91, 28.10.

2.3.3.2. Synthesis of T3B:

ε-BCL (400 mg, 1.55 mmol), T3 (26 mg, 0.052 mmol), and $Sn(Oct)_2$ (8 μL, 0.026 mmol) were taken in a Schlenk tube and subjected to polymerization for 6 hours. Yield – 230 mg (54%).

^1H NMR (400 MHz, $CDCl_3$) δ 7.13 – 7.04 (m, 10H), 7.03 – 6.96 (m, 7H), 6.92 (d, J = 8.6 Hz, 2H), 6.63 (d, J = 8.7 Hz, 2H), 4.54 (s, 2H), 4.21 – 4.03 (m, 80H), 3.77 – 3.56 (m, 85H), 3.50 – 3.36 (m, 39H), 2.48 – 2.30 (m, 153H), 2.03 – 1.65 (m, 240H), 1.44 (s, 324H).

^{13}C NMR (101 MHz, $CDCl_3$) δ 173.50, 170.87, 80.59, 75.47, 64.80, 61.25, 36.48, 32.92, 29.69, 28.91, 28.10.

2.3.3.3. Synthesis of T4B:

ε-BCL (950 mg, 3.68 mmol), T4 (36.9 mg, 0.046 mmol), and $Sn(Oct)_2$ (7 μL, 0.022 mmol) were taken in a Schlenk tube and subjected to polymerization for 10 hours. Yield – 400 mg (41%).

^1H NMR (400 MHz, $CDCl_3$) δ 6.93 (d, J = 8.0 Hz, 11H), 6.66 (d, J = 8.6 Hz, 8H), 4.42 (s, 7H), 4.22 – 4.04 (m, 96H), 3.78 – 3.55 (m, 113H), 3.49 – 3.37 (m, 46H), 2.43 (t, J = 6.4 Hz, 88H), 2.41 – 2.30 (m, 104H), 1.96 – 1.67 (m, 210H), 1.44 (s, 409H).

^{13}C NMR (101 MHz, $CDCl_3$) δ 173.49, 170.87, 80.58, 75.46, 64.80, 64.62, 61.25, 36.48, 32.92, 29.69, 28.91, 28.10.

2.3.3.4. Synthesis of T6B:

ε-BCL (950 mg, 3.68 mmol), T6 (36 mg, 0.052 mmol), and Sn(Oct)$_2$ (8 µL, 0.026 mmol) were taken in a Schlenk tube and subjected to polymerization for 12 hours. Yield – 600 mg (61%).

^{1}H NMR (400 MHz, CDCl$_3$) δ 7.12 – 7.04 (m, 6H), 7.03 – 6.87 (m, 9H), 6.67 – 6.58 (m, 4H), 4.54 (d, J = 9.6 Hz, 4H), 4.19 – 4.01 (m, 97H), 3.79 – 3.55 (m, 109H), 3.49 – 3.37 (m, 47H), 2.43 (t, J = 6.3 Hz, 99H), 2.40 – 2.31 (m, 96H), 1.97 – 1.66 (m, 288H), 1.44 (s, 427H).

^{13}C NMR (101 MHz, CDCl$_3$) δ 173.50, 170.87, 80.59, 75.47, 64.80, 61.25, 36.48, 32.92, 29.69, 28.91, 28.10.

2.3.3.4. Synthesis of T8B:

ε-BCL (950 mg, 3.68 mmol), T8 (42.6 mg, 0.046 mmol), and Sn(Oct)$_2$ (60 µL, 0.184 mmol) were taken in a Schlenk tube and subjected to polymerization for 14 hours. Yield – 718 mg (72.3%).

^{1}H NMR (400 MHz, CDCl$_3$) δ 6.99 – 6.85 (m, 9H), 6.73 – 6.59 (m, 8H), 4.41 (s, 8H), 4.27 – 4.03 (m, 174H), 3.83 – 3.53 (m, 195H), 3.52 – 3.36 (m, 84H), 2.50 – 2.26 (m, 349H), 1.92 – 1.65 (m, 385H), 1.44 (s, 770H).

^{13}C NMR (101 MHz, CDCl$_3$) δ 173.50, 170.86, 80.58, 75.46, 64.80, 61.24, 36.48, 32.93, 29.69, 28.91, 28.10.

2.3.4. Boc-deprotection of the TPE-BPCL homopolymers:

General procedure: 200mg of the required TPE boc-protected polymers are dissolved in 2 mL DCM. This setup is now taken in an ice bath, after which TFA (2 mL) is added slowly to this mixture and stirred for at least 30 minutes. TFA is then evaporated from the reaction mixture by repeated rounds (4-5 times) of DCM addition and partial removal by rotavap (DCM/TFA form an azeotrope). The approximately 1 mL DCM reaction mixture is then transferred to 25 mL of Et$_2$O:Hexane (1:1 v/v). The solvent is then decanted, and the precipitated polymer is adequately dried.

2.3.4.1. Synthesis of T2C:

T2C (200 mg) was dispersed in DCM, and TFA was added in an ice bath. TFA was removed after 30 minutes, and the reaction mixture was precipitated in Et$_2$O:Hexane to yield the deprotected polymer (150 mg). ^{1}H NMR (400 MHz, DMSO) δ 6.74 (dd, J = 14.5, 8.4 Hz, 1H), 4.05 (q, J = 6.8, 6.0 Hz, 10H), 3.57 (td, J = 6.1, 2.6 Hz, 12H), 2.37 (dt, J = 30.9, 6.8 Hz, 14H), 1.69 (qq, J = 14.7, 7.3 Hz, 16H).

2.3.4.2. Synthesis of T3C:

T3C (200 mg) was dispersed in DCM, and TFA was added in an ice bath. TFA was removed after 30 minutes, and the reaction mixture was precipitated in Et$_2$O:Hexane to yield the deprotected polymer (160 mg). ^{1}H NMR (400 MHz, DMSO) δ 12.13 (s, 4H), 7.11 (s, 1H), 6.96 (q, J = 8.1, 7.1 Hz, 1H), 5.75 (s, 1H), 4.17 − 4.11 (m, 1H), 4.04 (dh, J = 11.8, 6.8, 6.3 Hz, 8H), 3.56 (tq, J = 5.8, 3.3 Hz, 8H), 3.46 − 3.35 (m, 1H), 3.38 (s, 3H), 2.40 (t, J = 6.1 Hz, 8H), 2.32 (t, J = 7.6 Hz, 8H), 2.24 (s, 1H), 1.69 (hept, J = 7.2, 6.0 Hz, 11H), 1.24 (s, 1H), 0.89 − 0.77 (m, 1H).

2.3.4.3. Synthesis of T4C:

T4C (200 mg) was dispersed in DCM, and TFA was added in an ice bath. TFA was removed after 30 minutes, and the reaction mixture was precipitated in Et$_2$O:Hexane to yield the deprotected polymer (150 mg). ^{1}H NMR (400 MHz, DMSO) δ 12.14 (s, 43H), 6.86 (d, J = 8.3 Hz, 8H), 6.73 (d, J = 8.4 Hz, 8H), 4.04 (q, J = 7.7, 6.3 Hz, 91H), 3.56 (td, J = 6.1, 2.6 Hz, 88H), 2.36 (dt, J = 31.0, 6.8 Hz, 168H), 1.68 (tq, J = 14.6, 7.5, 6.1 Hz, 169H).

2.3.4.4. Synthesis of T6C:

T6C (200 mg) was dispersed in DCM, and TFA was added in an ice bath. TFA was removed after 30 minutes, and the reaction mixture was precipitated in Et$_2$O:Hexane to yield the deprotected polymer (165 mg). ^{1}H NMR (400 MHz, DMSO) δ 12.14 (s, 2H), 5.75 (s, 1H), 4.04 (tq, J = 11.7, 6.6 Hz, 4H), 3.56 (tq, J = 5.8, 3.3 Hz, 4H), 3.48 − 3.36 (m, 2H), 3.17 (s, 1H), 2.40 (t, J = 6.1 Hz, 4H), 2.31 (q, J = 8.7, 8.2 Hz, 4H), 1.68 (tq, J = 14.4, 7.2, 6.0 Hz, 5H), 1.24 (d, J = 5.6 Hz, 0H).

2.3.4.5. Synthesis of T8C:

T8C (200 mg) was dispersed in DCM, and TFA was added in an ice bath. TFA was removed after 30 minutes, and the reaction mixture was precipitated in Et_2O:Hexane to yield the deprotected polymer (155 mg). ^{1}H NMR (400 MHz, DMSO) δ 12.13 (s, 2H), 4.12 – 3.97 (m, 4H), 3.56 (td, J = 6.1, 2.4 Hz, 4H), 3.46 – 3 .35 (m, 2H), 2.40 (t, J = 6.1 Hz, 4H), 2.32 (t, J = 7.6 Hz, 4H), 1.81 – 1.56 (m, 6H), 1.24 (d, J = 5.6 Hz, 0H).

2.4. Self-assembly of the homopolymers:

5 mg of the polymer was dissolved in 0.5 mL of DMSO. 4.5 mL of Milli-Q water was taken in a vial, and the above solution was added dropwise into the vial over 15 minutes. Stirring was kept for 90 minutes, after which the contents were transferred into a semipermeable membrane (MWCO~3500). Dialysis was performed in water by replacing water at regular intervals of time.

2.5. Composition dependent studies:

2 mL solutions were made of DMSO:H_2O compositions varying from 100% H_2O to 0% H_2O, such that all samples contained the same concentration of the dialyzed polymer sample (0.1 mg/mL). Fluorescence measurement was taken for these samples at 340 nm excitation wavelength.

2.6. Concentration dependent studies:

DMSO dissolved polymer solutions were added to vials containing 2 mL water. Samples were prepared such that the solvent composition didn't vary much (%DMSO<2.5). The concentration of the polymers in the vials varied from 0.005 mg/mL to 0.1 mg/mL. Fluorescence measurement was taken at 340 nm excitation wavelength.

2.7. Doxorubicin encapsulation:

DOX encapsulation was carried out by the dialysis method. Doxorubicin hydrochloride (0.5 mg) was dissolved in 200 μL DMSO. A few drops of triethylamine were added for

neutralization. The DOX solution was added to the DMSO dissolved polymer sample (5 mg in 600 μL) and sonicated for 2-3 minutes. This solution was added dropwise to 4.2 mL water over 15 minutes, and stirred for 4 hours. The contents were transferred into a semipermeable membrane (MWCO~3500) and kept for dialysis. Water was replaced periodically to facilitate the movement of DMSO out of the membrane. DLC and DLE were calculated with the below equations:

$$DLC = \left(\frac{Weight\ of\ encapsulated\ drug}{Weight\ of\ polymer}\right) \times 100\%$$

$$DLE = \left(\frac{Weight\ of\ encapsulated\ drug}{Weight\ of\ drug\ in\ feed}\right) \times 100\%$$

The amount of DOX loaded can be calculated from Beer-Lambert's law:

$$A = \varepsilon c l$$

ε (molar absorptivity) for DOX is known, l (path length of light) is 1 cm for the cuvette being used, and the value of A (absorbance) can be obtained by carrying out absorption measurement for the dialyzed sample. In this way, we can calculate c, the concentration of DOX in our sample. This can now be utilized to calculate DLC and DLE for the polymer.

2.8. Cell viability assay:

The biocompatibility of the polymers was tested using the MTT assay. WT-MEF (wild type mouse embryonic fibroblast) cells were grown into a flask in the incubator with a humidified 5% CO_2 atmosphere at 37°C in DMEM (Dulbecco's modified eagle medium) containing 1% (v/v) penicillin-streptomycin and 10% (v/v) Fetal bovine serum. The cells were trypsinized, and a density of 1000 cells were seeded per well in a 96-well plate and incubated for 24 h at similar conditions. The media was replaced with fresh media containing different concentrations (10 to 80 ug/mL) of polymers and incubated for 72h. A column of wells was only added with fresh media and kept as control. After the incubation period, the media was aspirated, and 100 μL of MTT (3-(4,5-Dimethylthiazol-2-yl)-2,5-diphenyltetrazolium bromide) solution was added to each well and again incubated for 4 more hours followed by aspiration of media and addition of 100μL DMSO. The absorbance in each well at 570 nm was measured using

a Varioskan plate reader. A similar experiment was carried out for four of the DOX-loaded polymer solutions (T2C, T4C, T6C, T8C). The polymer solutions were taken such that they contained 0.1, 0.2, 0.4, 0.6, 0.8, and 1 µg/mL of doxorubicin. The control wells were loaded with corresponding concentrations of free doxorubicin.

The assay works in the following manner: MTT is a dye that undergoes reduction by mitochondrial oxidoreductase enzymes to generate a compound called formazan, whose absorbance can be measured to get a readout of the cell viability relative to the control where only media is provided. Since formazan is water soluble, it forms crystals in the aqueous medium. Thus, the next procedure involves the aspiration of media and addition of DMSO. DMSO dissolves the crystals, after which the absorbance reading can be taken. MTT reduction by the cellular enzymes yields formazan, and enzymatic machinery will be functioning only in living cells. Thus, higher absorbance corresponding to formazan implies a higher amount of MTT reduction, which further implies higher cell viability in the corresponding well. The cell viability of the polymer-loaded wells is compared with respect to the control wells having been incubated with only media.

2.9. Cellular uptake studies:

Cellular uptake of the polymers was demonstrated in the wild-type MEF cell line. A 6-well plate was taken, and 10^5 cells were seeded in each well containing flame-dried coverslip. The plate was incubated for 24 hours at 37°C in a 5% CO_2 environment in complete DMEM media. The media was then replaced with TPE-polymer solutions (200 µg/mL polymer concentration) in complete DMEM media. The wells were incubated for 6 hours, after which the media was aspirated, and the coverslips were cleaned twice with 1 mL PBS buffer. 4% paraformaldehyde solution in PBS was added and kept for 15 minutes at room temperature to fix the cells. PBS washing was performed, and the wells were incubated for 15 minutes after the addition of phalloidin green. Now, the coverslips were mounted on glass slides using 70% glycerol in water. After drying of the mounting medium, the cells were visualized using λ = 405 nm (TPE channel) and λ = 488 nm (phalloidin green channel) with a Leica SP8 confocal microscope and analyzed by ImageJ software.

3. Results and Discussion

3.1. Initiator synthesis:

A facile, multistep synthesis route was followed to get the targeted fluorescent initiators. Primary alcohols are ideal initiators for the tin-mediated ROP mechanism. Hence, the TPE molecules were derivatized to create a library of compounds with varying primary alcohol groups.

McMurry reaction between benzophenone and 4-hydroxybenzophenone resulted in TPE-1-OH and TPE-2-OH. These were subsequently reacted with ethyl chloroacetate to yield the corresponding ethyl ester products TPE-1-ester and TPE-2-ester. TPE-1-ester was reacted with tris base with methanol as solvent under reflux conditions to give the T3 initiator having three primary alcohol groups. TPE-2-ester was reacted with ethanolamine and tris base to give derivatives having two and six primary alcohol groups respectively (T2 and T6).
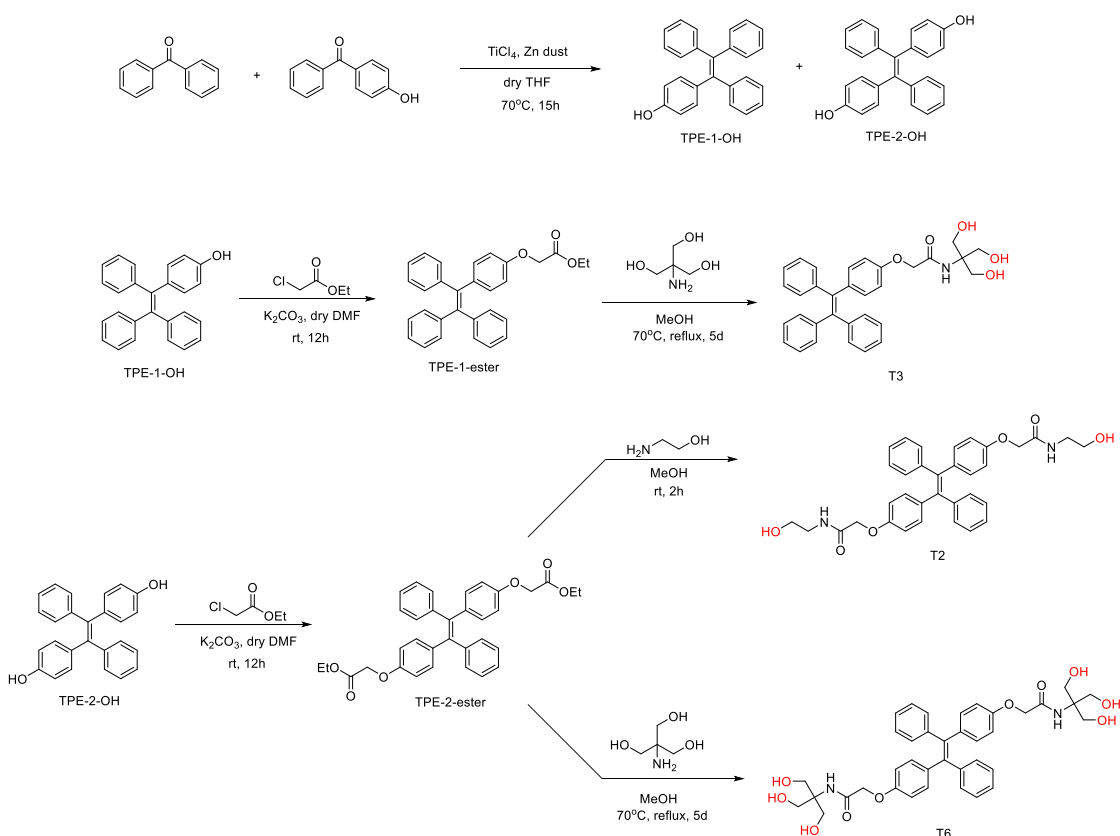

Figure 6: Reaction scheme for the synthesis of T2, T3, and T6 initiators

The NMR data for each reaction step is given below. The pattern of the aromatic peaks and the relative integration intensities confirm the formation of TPE-1-OH. The OH-substituted benzene ring is more electron rich, so the four protons (**a** and **g**) of this ring come more upfield in the NMR spectrum. The **a** protons are ortho to the OH group and hence are most electron rich. The reaction with ethyl chloroacetate is confirmed by three new peaks (**b**, **j**, **k**) with the proton shift and coupling corresponding to the ethyl and OCH_2 moieties. The formation of T3 from TPE-1-ester is confirmed by the absence of the ethyl peaks (**j**, **k**), the appearance of amide N-H peak (**c**), and upfield shifting of the **b** peak (amide carbonyl is less electron withdrawing than that of ester).
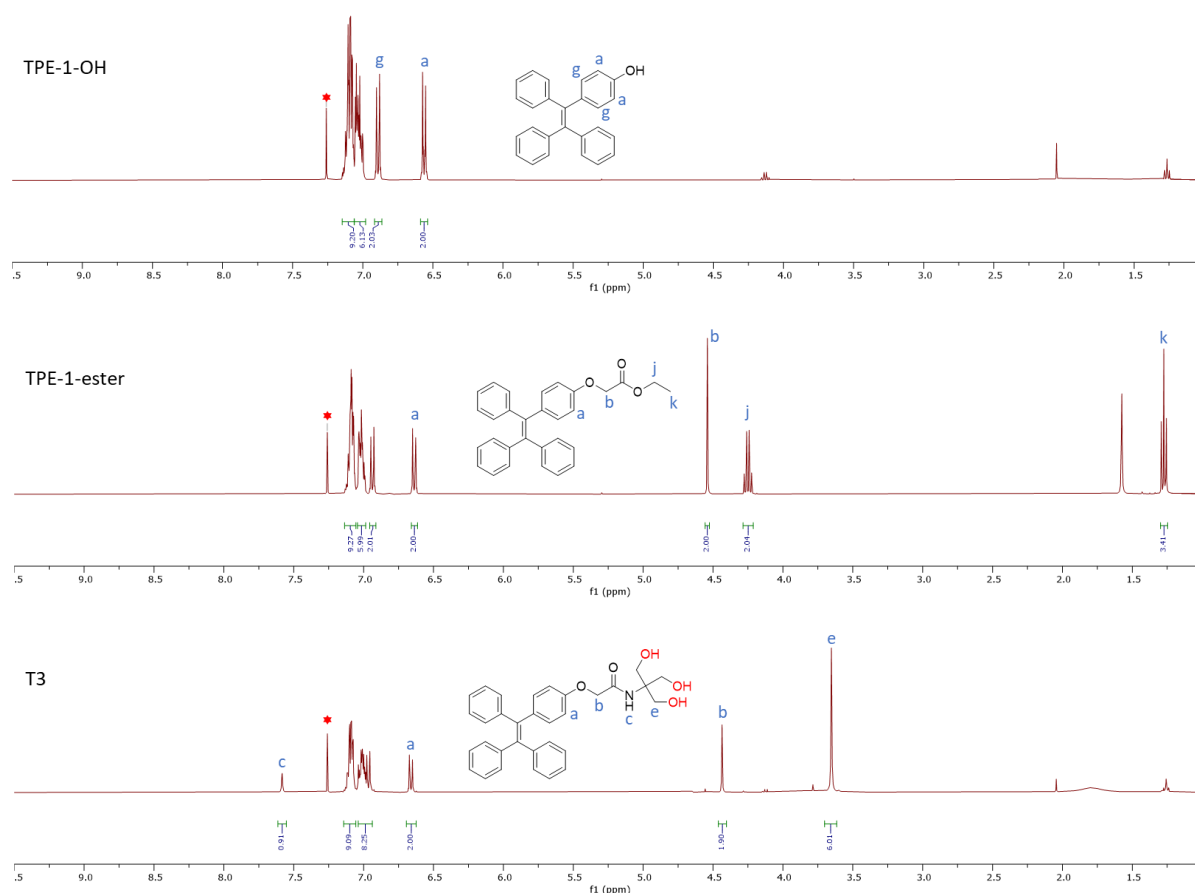

Figure 7: ^{1}H-NMR spectra for the synthesis of T3

The formation of T2 and T6 was confirmed similarly. Integrating the **d**, **e**, and **f** peaks with respect to **b** and **c** peaks confirms the formation of the TPE derivatives with two and six primary alcohol groups. Also, the doubling of peaks (eg, two peaks for **i**) is observed since our derivatives comprise a cis and trans mixture of products.
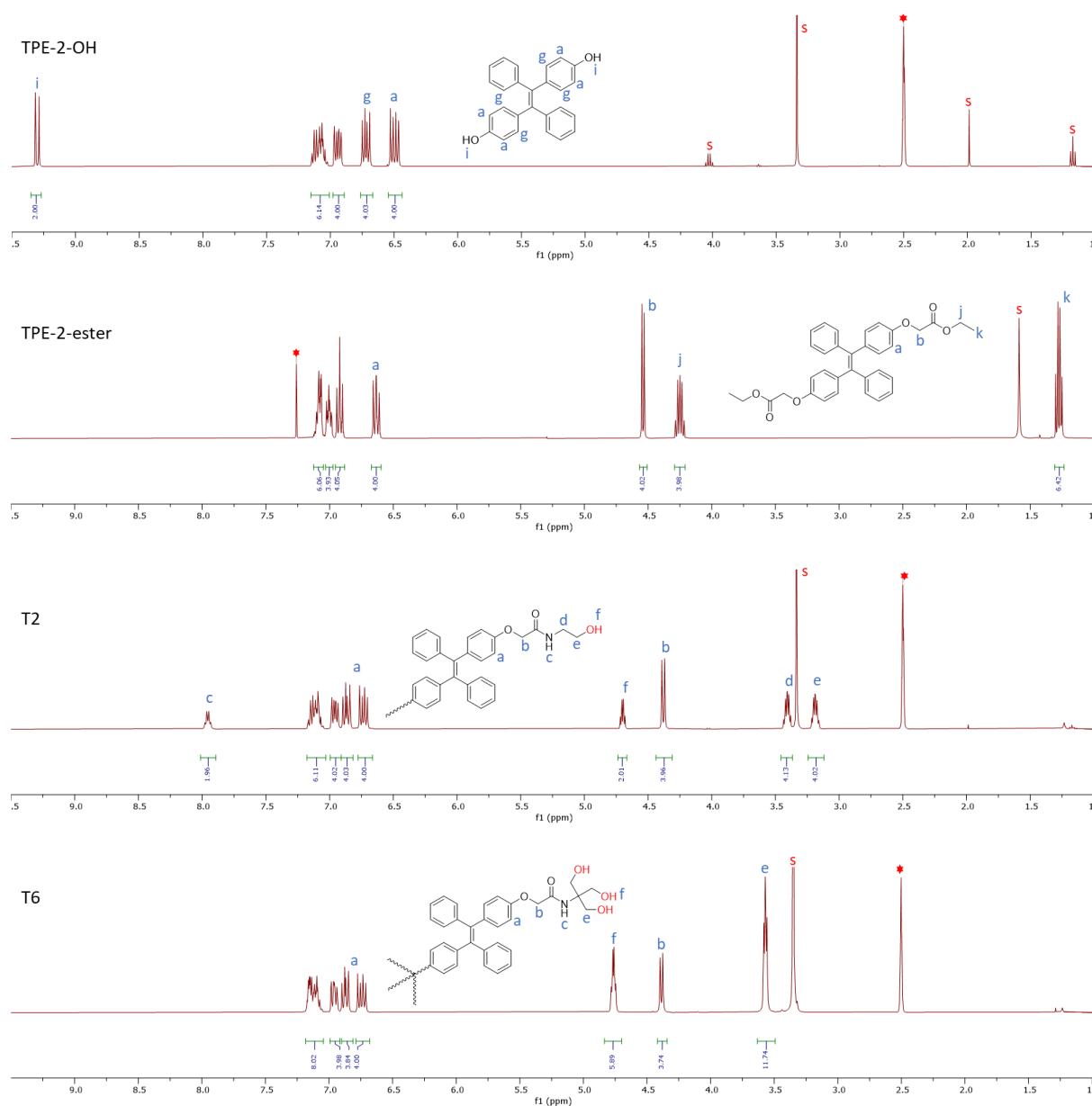
Figure 8: ^{1}H-NMR spectra for the synthesis of T2 and T6

Direct McMurry coupling of 4,4'-dihydroxybenzophenone unexpectedly resulted in many side products. The required product (TPE-4-OH) could not be isolated. Thus, the procedure by[27] was followed for the synthesis. 4,4'-dihydroxybenzophenone was first methylated, followed by self-coupling by McMurry reaction to give TPE-4-OMe. Methyl deprotection subsequently yielded TPE-4-OH. The corresponding tetra-ester was synthesized using ethyl chloroacetate. Reaction with ethanolamine and serinol yielded the T4 and T8 initiators, respectively.
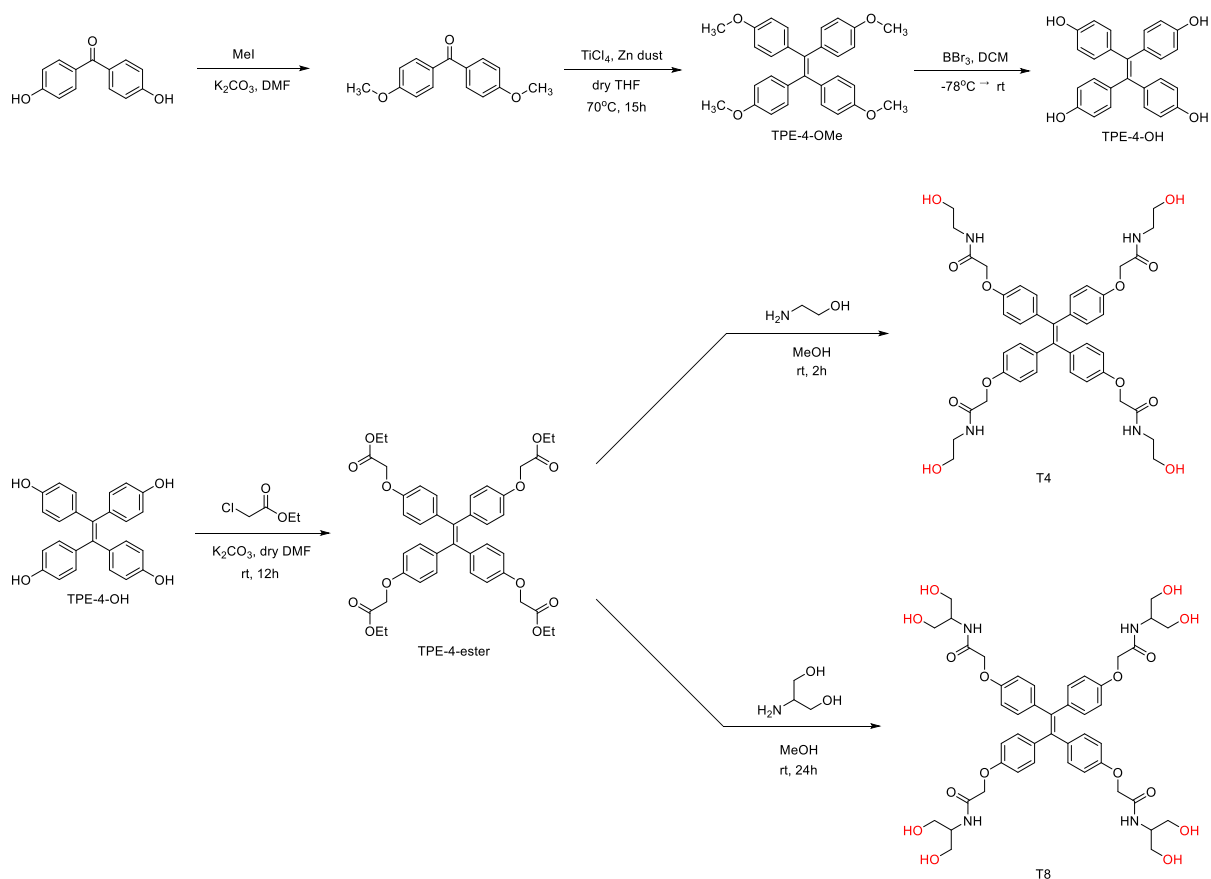
Figure 9: Reaction scheme for the synthesis of T4 and T8 initiators

The first methylation step was confirmed by the presence of the phenoxy methyl proton peak at δ3.89 ppm. The reductive coupling in the following step results in the TPE moiety which can be confirmed by the drastic upfield shift in the g and a protons due to the absence of the electron withdrawing carbonyl group, along with the relative integration values of the methyl with a and g protons. The disappearance of the methoxy peak confirms TPE-4-OH formation. Analysis for the subsequent steps for T4 and T8 synthesis follows similar to that of the previous initiators.

^{1}H-NMR analysis shows that the initiators are highly pure and thus are ideal for polymerization. The pattern of the aromatic hydrogens informs us of the symmetry of the TPE core, and the integration values of the b, c, d, e, and f protons confirm the presence of the desired initiators. The star symbol in the graphs denotes the deuterated solvent peak (CDCl₃ (δ7.26 ppm) or DMSO-d₆ (δ2.5 ppm)), while the s-marked peaks denote solvent impurities (which is H_2O in most of the cases).
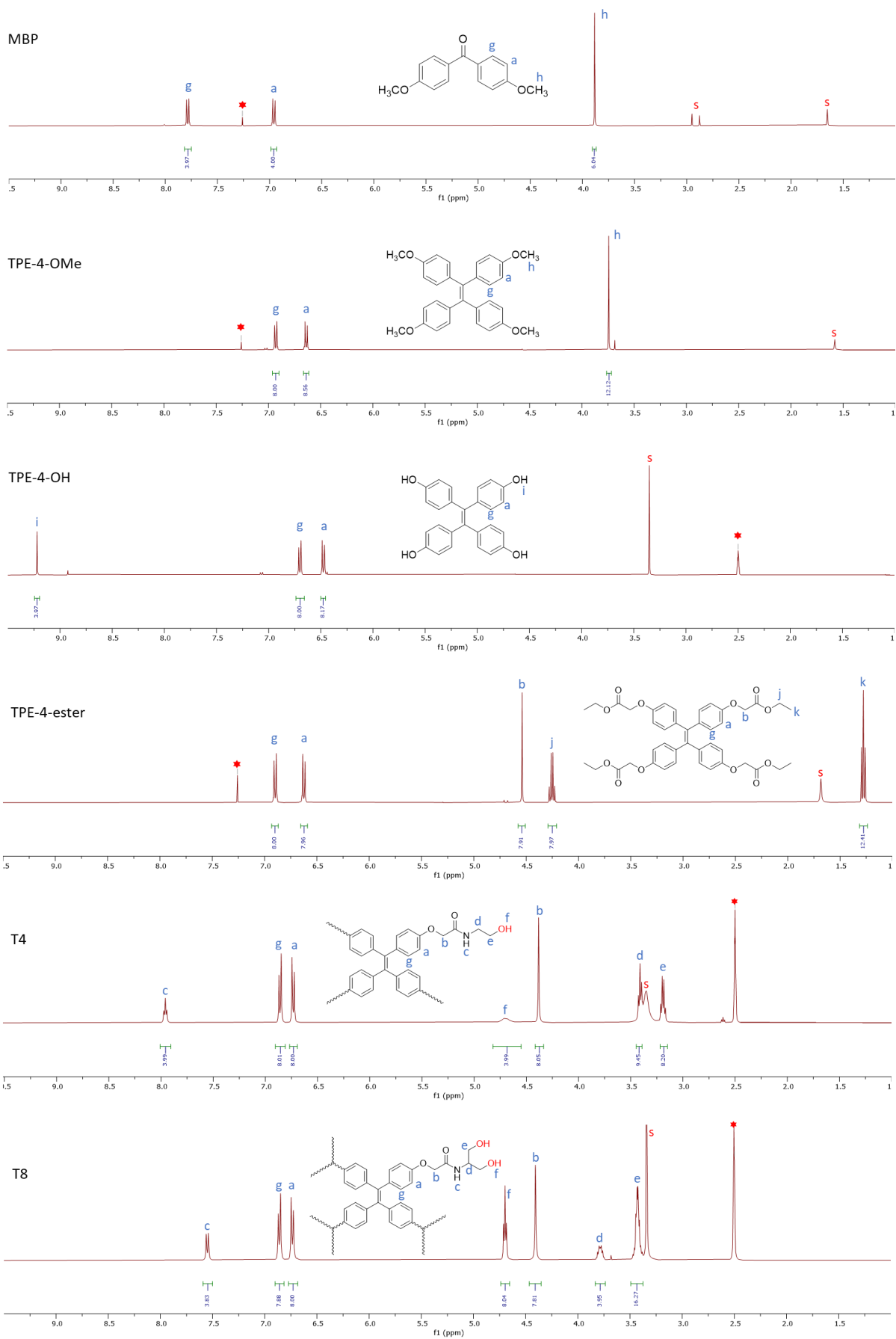
Figure 10: ^{1}H-NMR spectra for the synthesis of T4 and T8

3.2. Monomer synthesis:

A substituted caprolactone tert-butyl 3-((7-oxooxepan-4-yl)oxy)propanoate was synthesized following a known procedure[22]. The synthesis involves three steps: Mono-substitution of tert-butyl acrylate on the commercially available 1,4-cyclohexanediol, Oxidation of the unsubstituted alcohol, and Baeyer-Villiger oxidation.
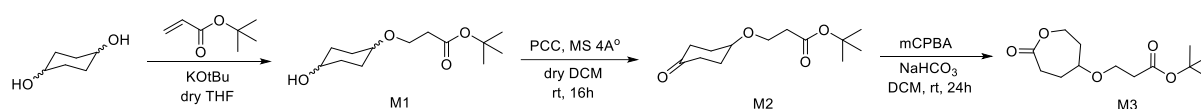

Figure 11: Reaction scheme for the synthesis of the Boc-caprolactone monomer

The product formation was confirmed by 1H-NMR. The cyclohexanediol used is a cis-trans mixture. Hence, the f proton in M1 is seen to have two peaks corresponding to the cis and trans products. The disappearance of the f peak in M2 confirms the successful oxidation. The appearance of g and g' peaks in the region of δ 4-4.5 ppm confirm the formation of the cyclic ester.
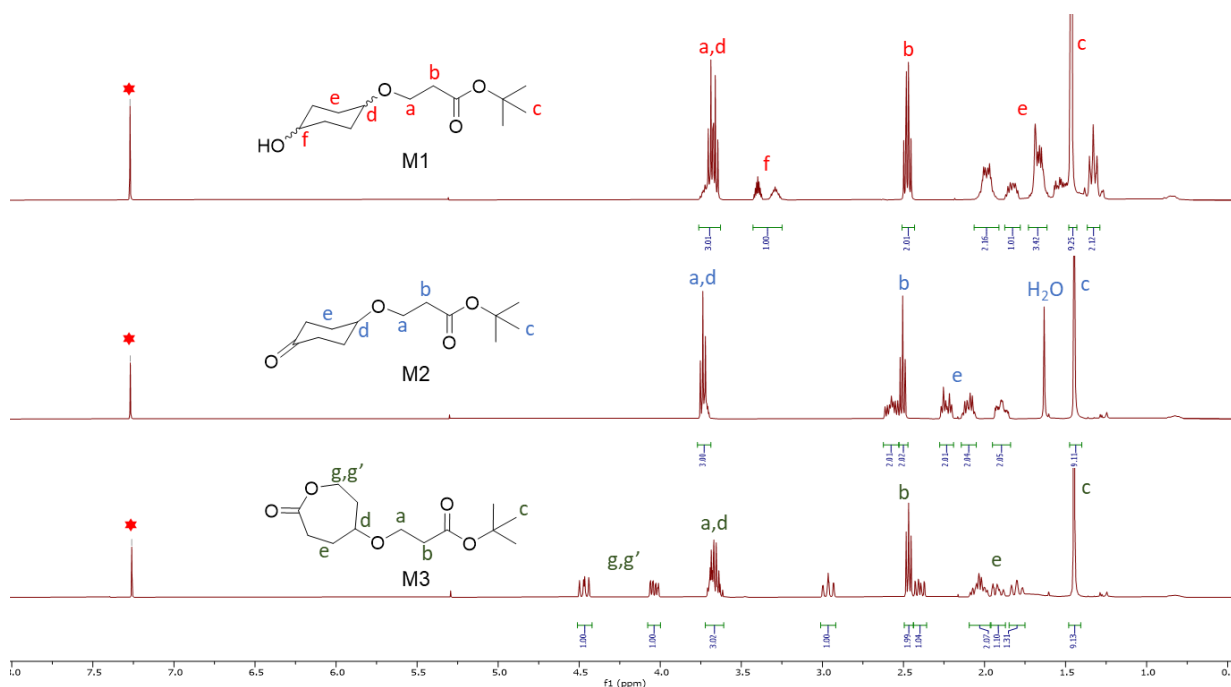

Figure 12: ¹H-NMR spectra for the synthesis of the Boc-caprolactone monomer
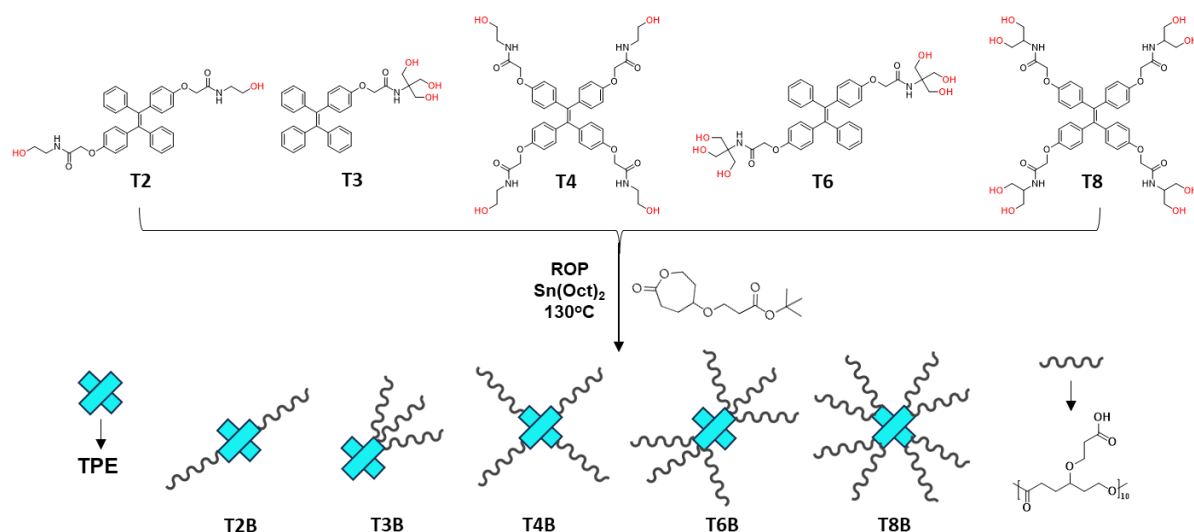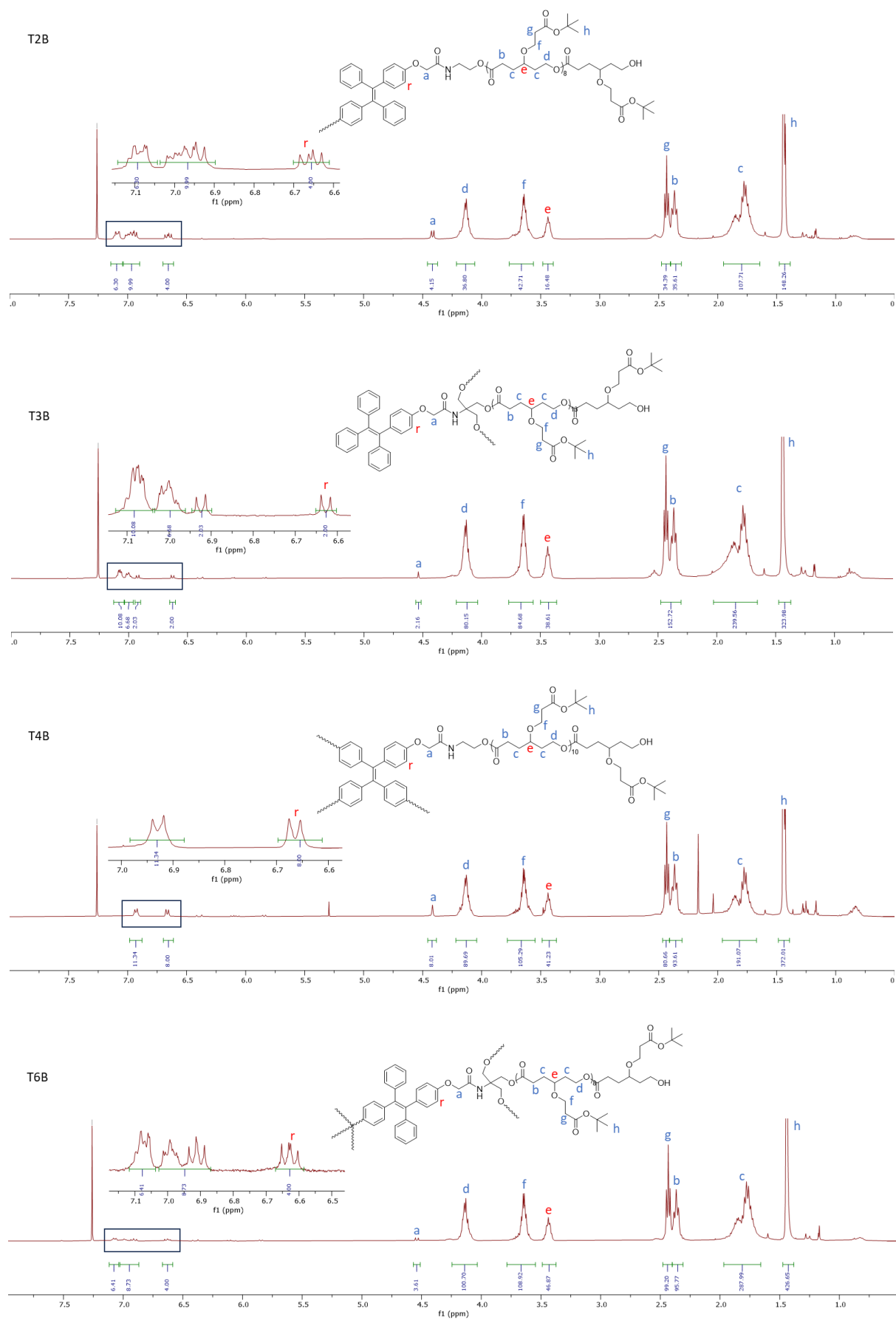
3.3. Polymer synthesis:

Figure 13: Synthesis of the TPE-conjugated polymers

With the initiators and monomer ready, ROP of the monomer was carried out in melt conditions with $Sn(Oct)_2$ catalyst. TGA analysis of the initiators was performed to ensure that the initiators were stable in the high-temperature reaction condition. Polymerization was performed, aiming M/I=10 for each arm. Pure polymers were obtained, which were characterized by ^{1}H-NMR and SEC. The degree of polymerization was calculated by comparing the integration of the **r** and **e** peaks for all the polymers. If we take the polymer T2B, for example, the **r** peak corresponds to two hydrogens of the initiator. Assigning the integration of the **r** peak as two units results in the integration value being one unit for one hydrogen. Integrating the **e** peak now gives the value of 16.4. The **e** peak corresponds to one hydrogen per monomer unit. This means that there are 16 monomer units incorporated. Assuming equal reactivity of the two initiating sites in the T2 initiator, we can say that, probabilistically, there are eight monomer units in each arm. The M/I obtained for the other polymers was calculated in a similar fashion.
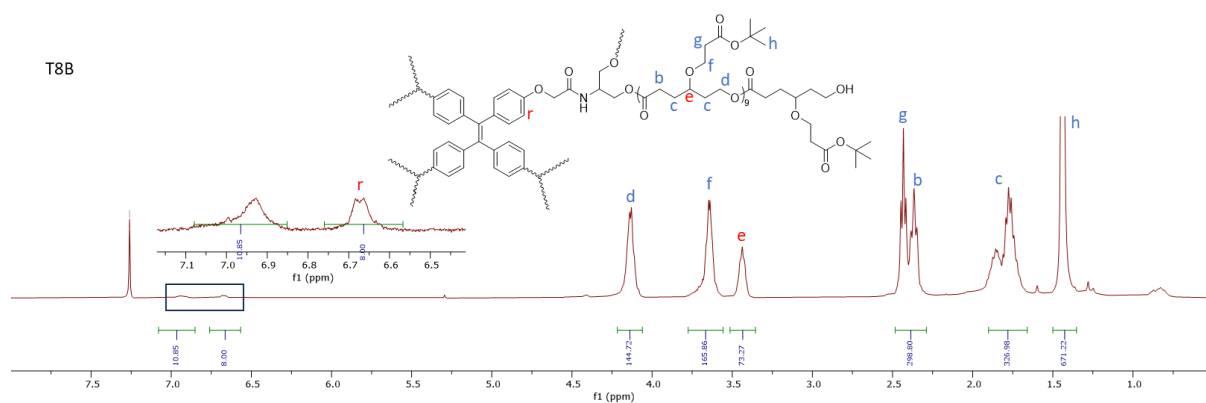
Figure 14: 1H-NMR spectra of the TPE-conjugated Boc-protected polymers

Subsequently, the Boc-protected polymers were deprotected using TFA to give the respective TPE-carboxy polymers. The synthesis of the Boc-protected polymer T8B from the 8-arm initiator T8, followed by the deprotection to get T8C, is shown in the below figure. Deprotection is confirmed by the disappearance of the Boc peak at 1.44 ppm. Deprotection of the other polymers was characterized similarly.

Figure 15: Synthesis of T8B and T8C

The table summarising the polymerizations shows that the number of monomer units incorporated is slightly less than what we aim for. All the polymers show narrow dispersity with monomodal distribution in SEC. The molec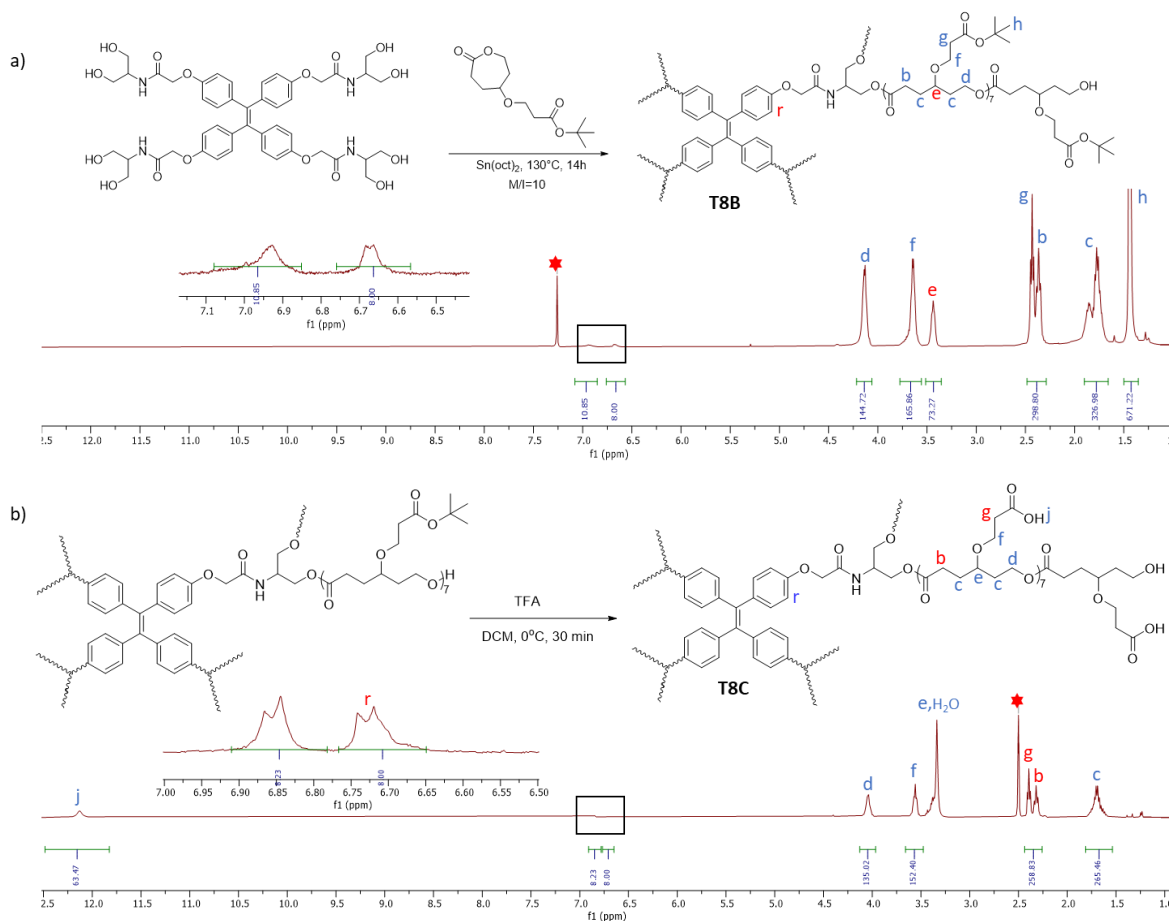ular weight is underestimated by SEC, which is possible because this value is dependent on the hydrodynamic volume of the polymers in the given solvent.
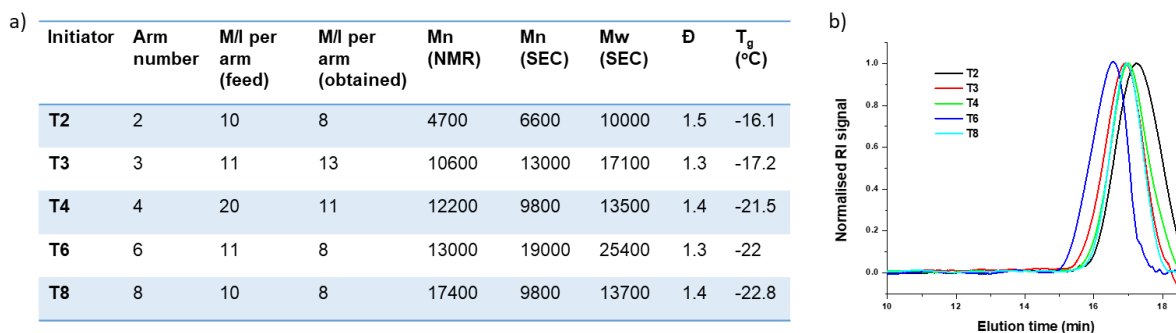
a)

Initiator	Arm number	M/I per arm (feed)	M/I per arm (obtained)	Mn (NMR)	Mn (SEC)	Mw (SEC)	Đ	T_g (°C)
T2	2	10	8	4700	6600	10000	1.5	-16.1
T3	3	11	13	10600	13000	17100	1.3	-17.2
T4	4	20	11	12200	9800	13500	1.4	-21.5
T6	6	11	8	13000	19000	25400	1.3	-22
T8	8	10	8	17400	9800	13700	1.4	-22.8

b)

Figure 16: NMR and SEC characterization of the polymers

(a) Table summarizing the degree of polymerization, M_n, M_w, PDI, and T_g for the TPE Boc-protected polymers; (b) SEC plots of the TPE Boc-protected polymers

TGA analysis of the polymers revealed that they are stable up to 200°C. Two distinct degradation steps can be observed in the TGA plots of the Boc-protected polymers: the first corresponds to the breaking of the Boc-ester (~195°C), while the second corresponds to the breaking of the backbone ester (~240°C). TGA of the deprotected polymers shows degradation directly after 240°C, thus re-confirming complete Boc deprotection. DSC analysis shows distinct T_g less than -16°C for all the Boc-protected polymers. The T_g curve is less prominent in the deprotected polymers.
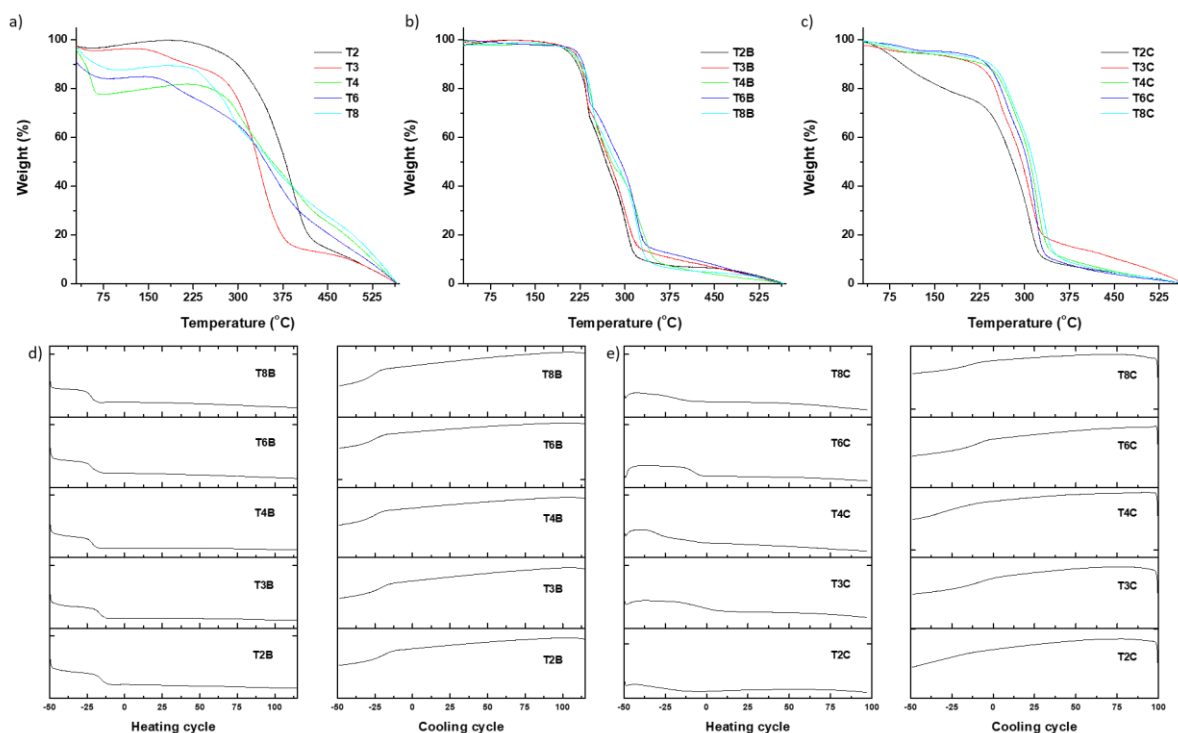
Figure 17: Thermal characterization of the polymers

TGA plots of (a) TPE initiators, (b) TPE Boc-protected polymers, and (c) TPE deprotected polymers; DSC plots showing the heating and cooling cycles for the (d) TPE Boc-protected polymers, and (e) TPE deprotected polymers.

3.4. Photophysical studies:

3.4.1. Initiator photoluminescence studies:

Absorbance measurements of the TPE initiators were taken. The absorption maximum is around 315 nm for all the initiators in 1% DMSO: 99% H_2O. In 100% DMSO, the absorption maximum of T4 and T8 are seen at 324 nm. The absorption measurements were also used to keep the OD (optical density) of all samples close to 0.1 so that any change in fluorescence intensity of these samples does not arise due to differences in absorption. As the synthesized initiators are derivatives of TPE, we expect them to exhibit AIE behaviour. The initiators were first dissolved in DMSO. Vials with different compositions of DMSO:H_2O were prepared, from 1% DMSO to 100% DMSO, into which the DMSO dissolved initiators were added. Fluorescence measurement showed that the TPE initiators fluoresce weakly in DMSO.
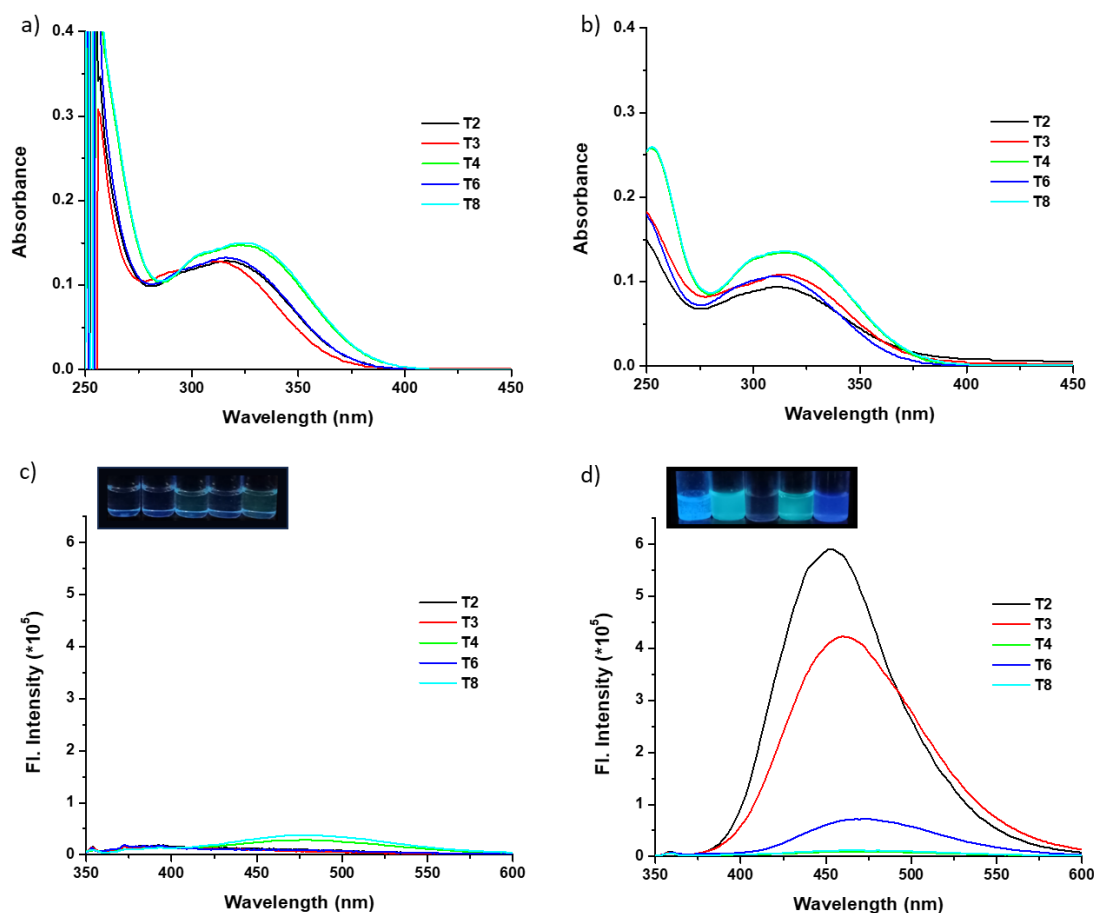
Figure 18: Absorption and fluorescence spectra of the TPE initiators

Absorbance of the TPE initiators in (a) 100% DMSO and (b) 1% DMSO: 99% H_2O;
Fluorescence of the TPE initiators in (c) 100% DMSO and (d) 1% DMSO: 99% H_2O

The fluorescence intensity was seen to suddenly spike after the water ratio increased beyond 70% for T3 and 80% for T2 and T6 (Figure 19f). This is the typical behaviour of AIEgens. Surprisingly, T4 and T8 didn't show emission enhancement even in 1% DMSO. Thus, these TPE derivatives do not exhibit AIE phenomenon in the DMSO:H_2O system. We propose that the high number of amide and alcohol groups surrounding the TPE moiety have a role to play in how these molecules interact with each other and prevent the expected AIE activity of these molecules.
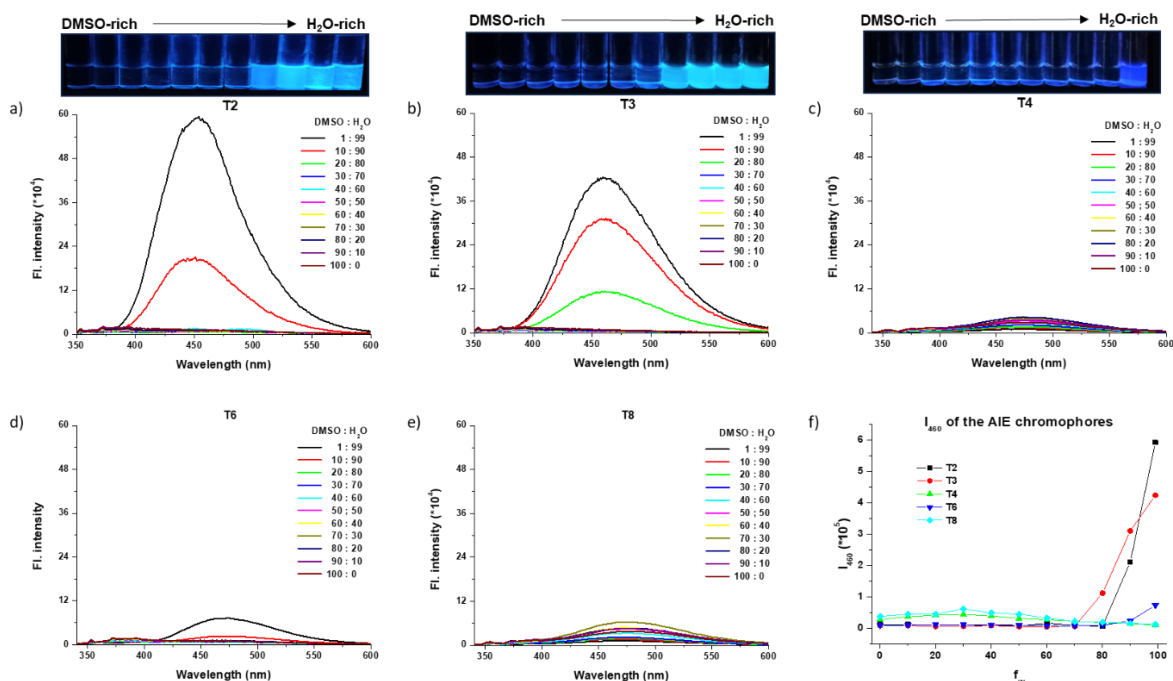
Figure 19: Composition dependent fluorescence study on the TPE initiators

Composition dependent luminescence of the initiators (a) T2, (b) T3, (c) T4, (d) T6, and (e) T8; (f) Demonstration of AIE by plotting of intensity at emission maximum (I_{em}) versus f_w

3.4.2. Polymer photoluminescence studies:

Firstly, concentration dependent studies were undertaken on the TPE-CPCL polymers (Figure 22). Plotting the intensity at emission maxima versus the chromophore concentration revealed the following order for the polymers: T4C>T8C>T6C>T2C>T3C. This means that for a particular TPE concentration, the T4C sample fluoresces more than, say, T6C, which means the AIE effect in T4C is higher than in T6C. It is interesting to notice that the order follows the amount of substitution at the TPE core. T4C and T8C have the polymer chains growing on all four phenyl rings, while T6C and T2C have the chains growing from two phenyl rings, and the other two are free, while the T3C polymer will have three free phenyl rings. To monitor the AIE phenomenon, composition dependent studies were carried out by dissolving a fixed volume of the dialyzed sample in vials of different DMSO:H_2O compositions (Figure 21). The polymers show emission enhancement with an increase in f_w (Figure 21f). All five polymers, T2C, T3C, T4C, T6C, and T8C, showed 5-6 fold enhancement compared to their emission in 100% DMSO, which is shown in the I/I_o plot below.
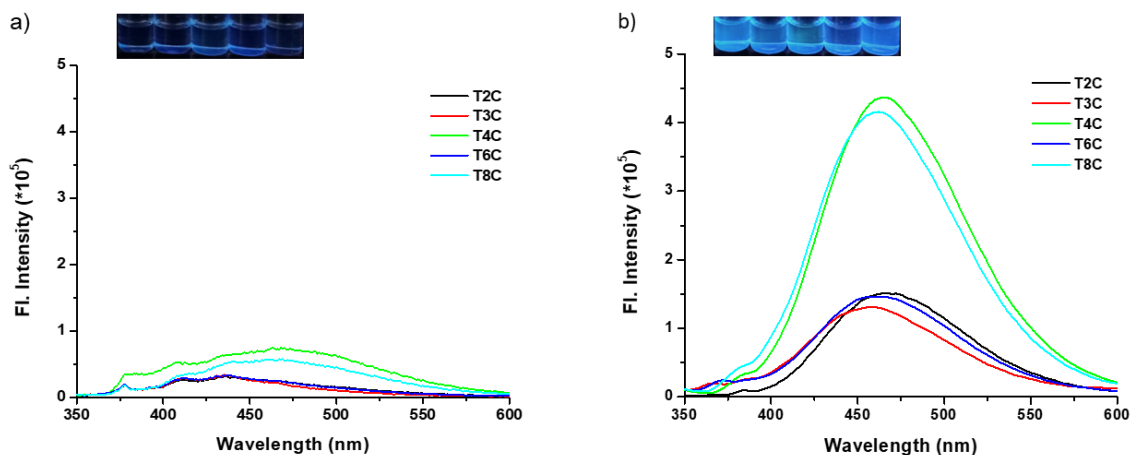
Figure 20: RIM of TPE core in action in the TPE-CPCL polymers

Fluorescence in (a) DMSO and (b) Water of the TPE-CPCL polymers. The effect of RIM is seen as an enhancement in emission intensity in H_2O compared to DMSO
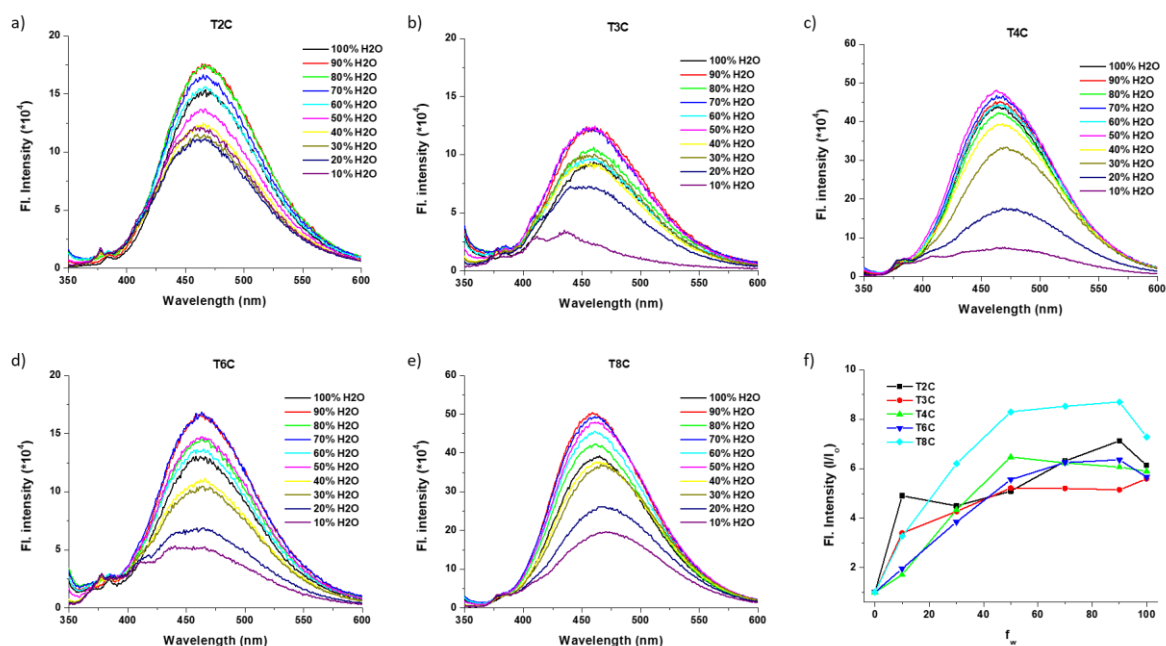

Figure 21: Composition dependent fluorescence studies on the TPE-CPCL polymers

Composition dependent fluorescence plots of self-assembled (a) T2C, (b) T3C, (c) T4C, (d) T6C, and (e) T8C polymers with varying DMSO:H_2O composition; (f) I/I_o plot for the TPE-CPCL polymers (I – Intensity at emission maximum (460nm), I_o – value of I in 100% DMSO) with fraction of water
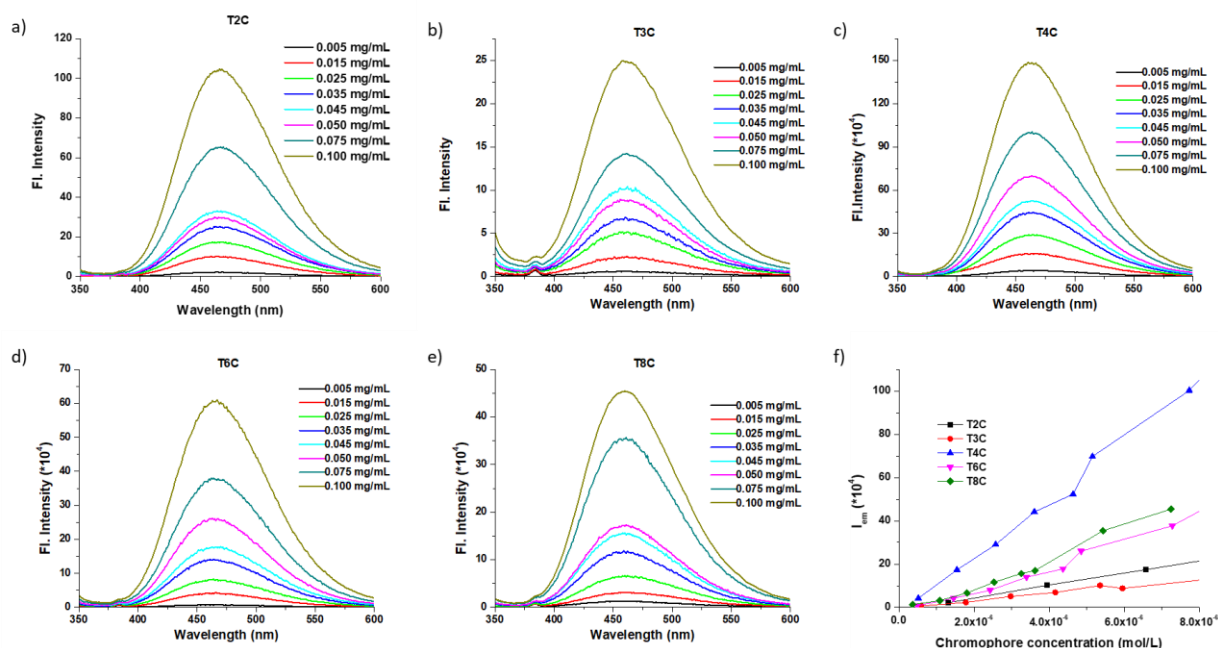
Figure 22: Concentration dependent fluorescence study on the TPE-CPCL polymers

Concentration dependent fluorescence study on (a) T2C, (b) T3C, (c) T4C, (d) T6C, and (e) T8C polymers; (f) I_{em} versus chromophore concentration plot for the different TPE-CPCL polymers

The emission activity of the T4C and T8C polymers is of special interest to us. While it is known that the polymer architecture can have a role in the emission intensity of the TPE core[21], this work demonstrates the **fluorescence turn-on** of non-emissive TPE derivatives achieved by polymerization. Given the structure of the T4C and T8C polymers, where the polymer chains of a given molecule surround the TPE core in all directions, it is highly unlikely that two TPE cores can come together in close proximity to aggregate. Thus, the plausible reason for TPE emission in these molecules is the steric hindrance of the polymer chains causing RIM of the TPE core and, thus, emission. Since we are starting with AIE-inactive TPE derivatives (T4 and T8), the TPE emission observed in the dialyzed polymer samples is entirely attributable to the RIM caused by the polymer chains. TPE derivatives such as T4 and T8 are ideal candidates to better understand the effect of polymerization (including degree of polymerization and the functionalities in the polymer chain) and polymer architecture on TPE emission.

3.5. Characterization of nanoparticles:

DLS of the self-assembled nanoparticles was carried out. The size (diameter) of the nanoparticles is in the range of 100-150nm. The size range indicates the formation of aggregated micelles.
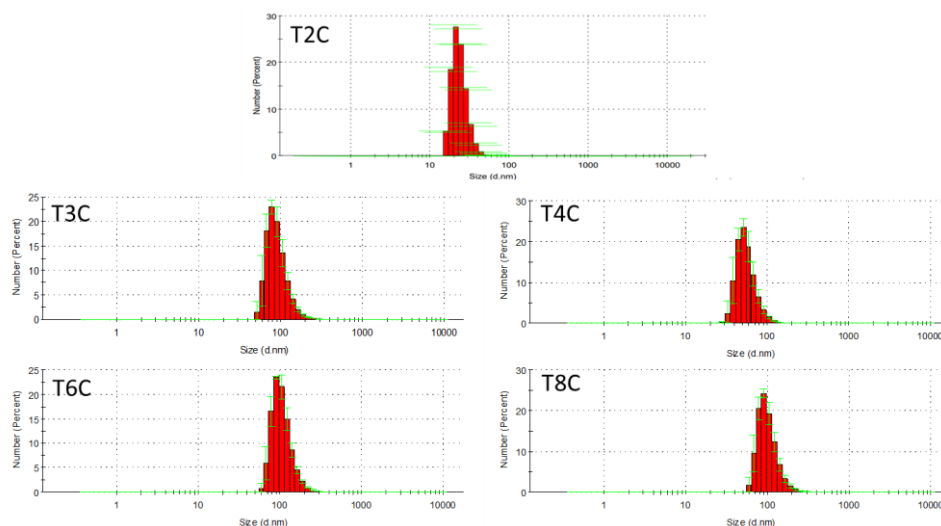
Figure 23: DLS measurement of the self-assembled TPE-CPCL polymers

Dilution dependent studies were conducted on two polymers, T3C and T8C, to monitor the aggregation property. Initially, the polymer samples show a size of ~100nm. But as the concentration becomes low, the sudden transition from aggregated micelles to individual nanoparticles takes place. For both polymers, this happened at the concentration of 0.001 mg/mL. We can thus conclude that 0.001 mg/mL is the critical aggregation concentration for both these polymers.

Figure 24: Dilution dependent DLS studies on T3-CPCL and T8-CPCL

3.6. Doxorubicin encapsulation:

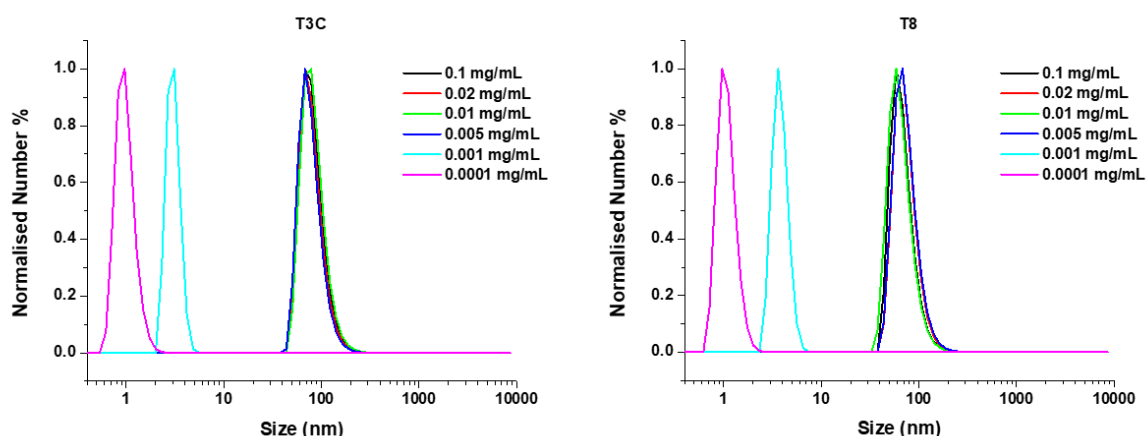To know our polymers' drug loading capabilities, two polymers T4C and T8C were loaded with DOX. This was done by dissolving the polymer and DOX in DMSO, mixing them together, and carrying out the self-assembly. Unloaded DOX and DMSO get out of the system during the dialysis process, and hence, only the DOX that has undergone successful loading will be present in the dialyzed sample.

Since both TPE and DOX are present in our system, the following processes are possible- 1) AIE of TPE on excitation of TPE at 340 nm; 2) Emission of DOX on excitation of TPE at 340 nm (FRET); 3) Fluorescence quenching between TPE and DOX. In order to investigate the nature of TPE-DOX interaction in our system, the OD of all the samples (polymer alone, DOX alone, and DOX-loaded polymer) was maintained at 0.1. The figure below shows the fluorescence plots of the dialyzed samples of T4C and T8C. The presence of DOX is confirmed by seeing DOX emission when the polymer sample is excited at 488 nm. However, when the sample is excited at 340 nm (the absorption wavelength for TPE), there is no DOX emission, indicating that the FRET phenomenon is absent. The emission intensity for both TPE (red curve) and DOX (green curve) in the DOX-loaded polymer sample is reduced compared to the TPE intensity in polymer alone (black curve) and DOX intensity in DOX alone (blue curve) samples, respectively. Thus, we can conclude that a partial quenching interaction is happening between the DOX and TPE moieties. The DLC and DLE for the polymers are tabulated in the below figure.

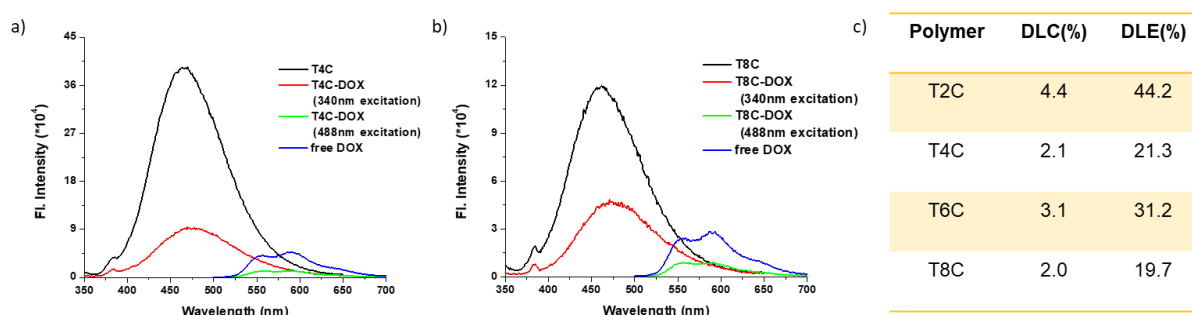| Polymer	DLC(%)	DLE(%)
T2C	4.4	44.2
T4C	2.1	21.3
T6C	3.1	31.2
T8C	2.0	19.7

Figure 25: DOX encapsulation study on the TPE-CPCL polymers

3.7. Cell viability assay:

The synthesized TPE polymers are made of aliphatic polyesters, which are known to be biocompatible and biodegradable (ref). The MTT assay reveals that all the polymers

are indeed biocompatible. All the polymers are found to be non-toxic up to 80 µg/mL. Thus, the biocompatibility of the polymers isn't hindered by the differences in molecular architecture in the polymers. For the DOX-loaded polymer samples, it is seen that the cell viability decreases with an increase in the drug-loaded polymer concentration. All the drug-loaded polymer solutions are able to kill the cells as effectively as the free drug. The IC_{50} of the drug-loaded polymers is observed to be between 0.6-0.8 µg/mL, while for the free drug, it is seen to be around 0.6 µg/mL. There is no noticeable role played by the molecular topology of the drug-loaded polymers on cell viability in the MTT assay.
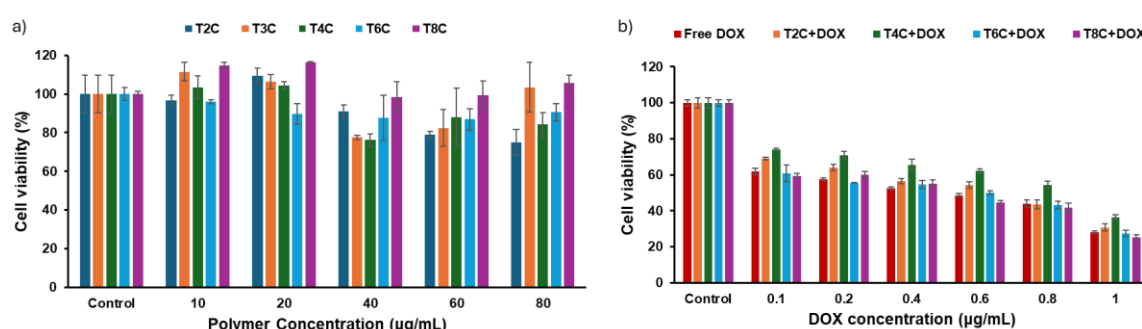

Figure 26: MTT assay

MTT assay carried out for a) The TPE-polymers T2C, T3C, T4C, T6C, and T8C; b) The drug-loaded nanocarriers of T2C, T4C, T6C and T8C

3.8. Cellular uptake studies:

Since our polymers contain the TPE moiety and are fluorescent in the self-assembled state, direct visualization of the polymers in biological systems is now possible. The cells have been visualized using the λ = 405nm and λ = 488nm channels corresponding to emission by TPE and phalloidin green, respectively. Phalloidin green stains the actin cytoskeleton of a cell, which is present throughout the cytoplasm. The last row, which corresponds to the merged image from both these channels, shows the colocalization of signals from TPE and phalloidin green. This demonstrates that the designed polymeric nanoparticles have been taken up by the cells. Also, there is no TPE emission coming from the plasma membrane in the merged images (characterized by the presence of only the red colour marked for phalloidin green). Additionally, there is an oval region in each of the cells, which is dark compared to its surroundings. This corresponds to the nucleus, which informs us that there is no

nuclear breach of the polymer nanoparticles. Thus, we can conclude that the polymeric nanocarriers are present mostly in the cytoplasm.
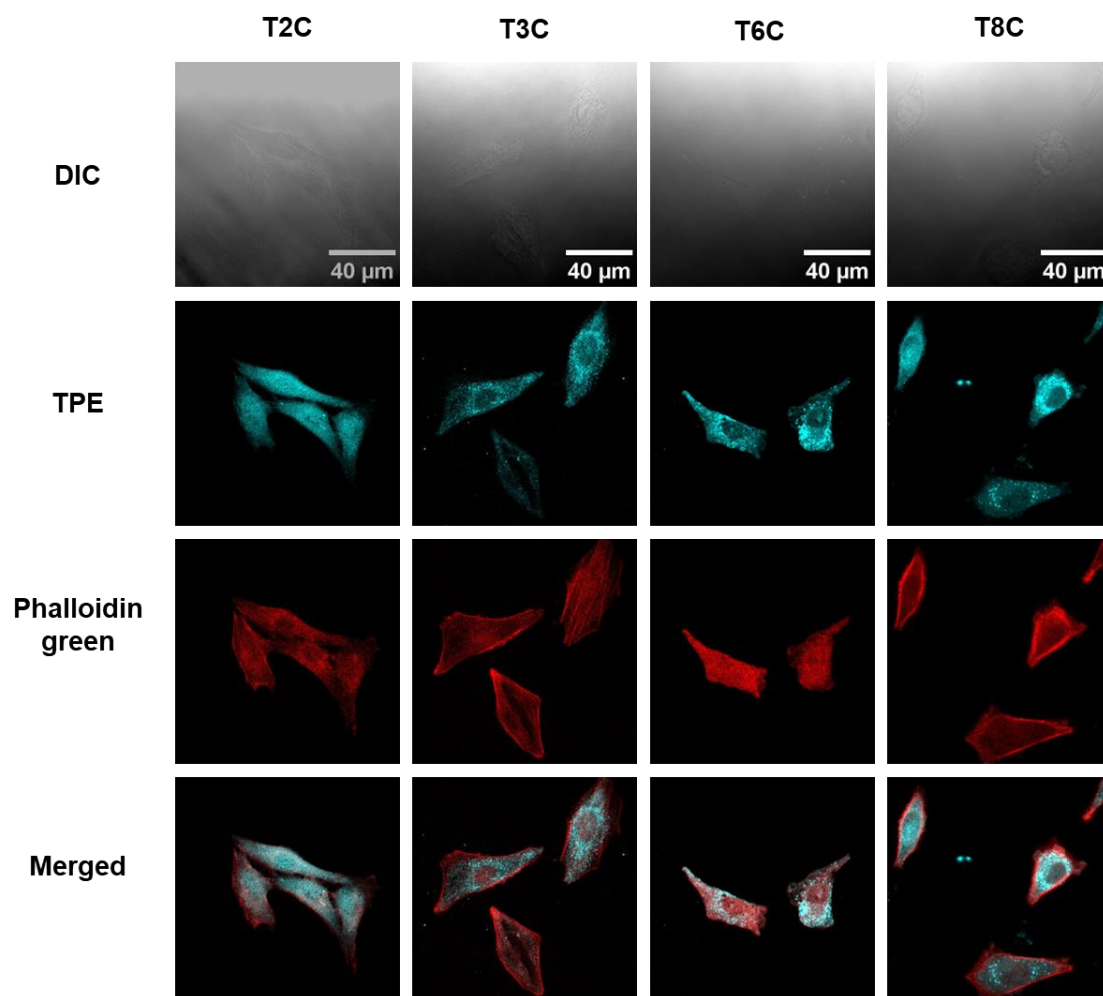

Figure 27: Cellular uptake studies

Cellular uptake of the self-assembled polymers after 6 h in WT-MEF cell line. TPE (blue channel) was imaged with λ_{ex} =405nm and λ_{em} =415-470nm. Phalloidin green was imaged with λ_{ex} =488nm and λ_{em} =498-600nm. The merged row denotes the merged image of the TPE and phalloidin green channels

4. Conclusion

In summary, we have successfully synthesized hydroxy-functionalized TPE initiators by multistep synthesis. Photoluminescence measurements on these initiators showed that T2, T3, and T6 are typical AIEgens. But surprisingly, T4 and T8 initiators didn't show emission enhancement in water. These initiators most likely have higher affinity to water compared to the other initiators, thus possibly resulting in no aggregation even in water. Star polymers were synthesized by the core-first approach through the ROP of Boc-substituted caprolactone. Upon deprotection of the Boc group, these polymers have a core-shell architecture with TPE as the hydrophobic core and the carboxy-substituted PCL as the hydrophilic shell. Self-assembly of these polymers resulted in nanoparticles with a size of 100-150 nm. All the self-assembled polymers are AIE active. The 3D polymer architecture, which is defined by the phenyl substitution of the TPE core in our case, seems to have an influence on the emission property of TPE. The following trend was observed in the emission enhancement of the polymers- the more the substitution, the higher the enhancement. Thermal analysis of the polymers revealed that the polymers are amorphous and stable till 240°C. DOX encapsulation for the polymers was carried out to assess their therapeutic ability. The polymers were observed to load at least 2% DOX. Cellular uptake studies in the WT-MEF cell line revealed uptake of polymer, confirmed by the visualization of TPE emission. The MTT assay showed that the polymers are non-toxic to cells, whereas the drug-loaded nanoparticles were able to kill cells as effectively as the free drug. The polymers have exciting prospects diagnostically- the change in TPE-DOX interaction can be tracked upon enzymatic degradation. The AIE intensity can also differ as the RIM of the TPE cores will change.

5. References

(1)   Senapati, S.; Mahanta, A. K.; Kumar, S.; Maiti, P. Controlled Drug Delivery Vehicles for Cancer Treatment and Their Performance. *Signal Transduct. Target. Ther.* **2018**, *3* (1), 1–19. https://doi.org/10.1038/s41392-017-0004-3.

(2)   Shi, J.; Kantoff, P. W.; Wooster, R.; Farokhzad, O. C. Cancer Nanomedicine: Progress, Challenges and Opportunities. *Nat. Rev. Cancer* **2017**, *17* (1), 20–37. https://doi.org/10.1038/nrc.2016.108.

(3)   Farokhzad, O. C.; Langer, R. Impact of Nanotechnology on Drug Delivery. *ACS Nano* **2009**, *3* (1), 16–20. https://doi.org/10.1021/nn900002m.

(4)   Iqbal, J.; Abbasi, B. A.; Ahmad, R.; Mahmood, T.; Ali, B.; Khalil, A. T.; Kanwal, S.; Shah, S. A.; Alam, M. M.; Badshah, H.; Munir, A. Nanomedicines for Developing Cancer Nanotherapeutics: From Benchtop to Bedside and Beyond. *Appl. Microbiol. Biotechnol.* **2018**, *102* (22), 9449–9470. https://doi.org/10.1007/s00253-018-9352-3.

(5)   Sun, Q.; Sun, X.; Ma, X.; Zhou, Z.; Jin, E.; Zhang, B.; Shen, Y.; Van Kirk, E. A.; Murdoch, W. J.; Lott, J. R.; Lodge, T. P.; Radosz, M.; Zhao, Y. Integration of Nanoassembly Functions for an Effective Delivery Cascade for Cancer Drugs. *Adv. Mater.* **2014**, *26* (45), 7615–7621. https://doi.org/10.1002/adma.201401554.

(6)   Matsumura, Y.; Maeda, H. A New Concept for Macromolecular Therapeutics in Cancer Chemotherapy: Mechanism of Tumoritropic Accumulation of Proteins and the Antitumor Agent Smancs. *Cancer Res.* **1986**, *46* (12 Pt 1), 6387–6392.

(7)   Fang, J.; Sawa, T.; Maeda, H. Factors and Mechanism of "EPR" Effect and the Enhanced Antitumor Effects of Macromolecular Drugs Including SMANCS. *Adv. Exp. Med. Biol.* **2003**, *519*, 29–49. https://doi.org/10.1007/0-306-47932-x_2.

(8)   Alasvand, N.; Urbanska, A. M.; Rahmati, M.; Saeidifar, M.; Gungor-Ozkerim, P. S.; Sefat, F.; Rajadas, J.; Mozafari, M. Chapter 13 - Therapeutic Nanoparticles for Targeted Delivery of Anticancer Drugs. In *Multifunctional Systems for Combined Delivery, Biosensing and Diagnostics*; Grumezescu, A. M., Ed.; Elsevier, 2017; pp 245–259. https://doi.org/https://doi.org/10.1016/B978-0-323-52725-5.00013-7.

(9)   Duncan, R. The Dawning Era of Polymer Therapeutics. *Nat. Rev. Drug Discov.* **2003**, *2* (5), 347–360. https://doi.org/10.1038/nrd1088.

(10)   Feng, H.; Lu, X.; Wang, W.; Kang, N. G.; Mays, J. W. Block Copolymers: Synthesis, Self-Assembly, and Applications. *Polymers (Basel).* **2017**, *9* (10). https://doi.org/10.3390/polym9100494.

(11)   Haag, R.; Kratz, F. Polymer Therapeutics: Concepts and Applications. *Angew. Chemie - Int. Ed.* **2006**, *45* (8), 1198–1215. https://doi.org/10.1002/anie.200502113.

(12)   Smart, T.; Lomas, H.; Massignani, M.; Flores-Merino, M. V.; Perez, L. R.; Battaglia, G. Block Copolymer Nanostructures. *Nano Today* **2008**, *3* (3–4), 38–46. https://doi.org/10.1016/S1748-0132(08)70043-4.

(13) Langer, R. Polymeric Delivery Systems for Controlled Drug Release. *Chem. Eng. Commun.* **1980**, *6* (1–3), 1–48. https://doi.org/10.1080/00986448008912519.

(14) Labet, M.; Thielemans, W. Synthesis of Polycaprolactone: A Review. *Chem. Soc. Rev.* **2009**, *38* (12), 3484–3504. https://doi.org/10.1039/b820162p.

(15) Chen, T.; Cai, T.; Jin, Q.; Ji, J. Design and Fabrication of Functional Polycaprolactone. *E-Polymers* **2015**, *15* (1), 3–13. https://doi.org/10.1515/epoly-2014-0158.

(16) Ren, J. M.; McKenzie, T. G.; Fu, Q.; Wong, E. H. H.; Xu, J.; An, Z.; Shanmugam, S.; Davis, T. P.; Boyer, C.; Qiao, G. G. Star Polymers. *Chem. Rev.* **2016**, *116* (12), 6743–6836. https://doi.org/10.1021/acs.chemrev.6b00008.

(17) Pranav, U.; Malhotra, M.; Pathan, S.; Jayakannan, M. Structural Engineering of Star Block Biodegradable Polymer Unimolecular Micelles for Drug Delivery in Cancer Cells. *ACS Biomater. Sci. Eng.* **2023**, *9* (2), 743–759. https://doi.org/10.1021/acsbiomaterials.2c01201.

(18) Blencowe, A.; Tan, J. F.; Goh, T. K.; Qiao, G. G. Core Cross-Linked Star Polymers via Controlled Radical Polymerisation. *Polymer (Guildf).* **2009**, *50* (1), 5–32. https://doi.org/10.1016/j.polymer.2008.09.049.

(19) Mei, J.; Leung, N. L. C.; Kwok, R. T. K.; Lam, J. W. Y.; Tang, B. Z. Aggregation-Induced Emission: Together We Shine, United We Soar! *Chem. Rev.* **2015**, *115* (21), 11718–11940. https://doi.org/10.1021/acs.chemrev.5b00263.

(20) Mei, J.; Hong, Y.; Lam, J. W. Y.; Qin, A.; Tang, Y.; Tang, B. Z. Aggregation-Induced Emission: The Whole Is More Brilliant than the Parts. *Adv. Mater.* **2014**, *26* (31), 5429–5479. https://doi.org/10.1002/adma.201401356.

(21) Wei, Z.; Chen, D.; Zhang, X.; Wang, L.; Yang, W. Precise Synthesis of Structurally Diverse Aggregation-Induced Emission-Active Polyacrylates by Cu(0)-Catalyzed SET-LRP with Macromolecular Structure-Correlated Emission. *Macromolecules* **2022**, *55* (7), 2911–2923. https://doi.org/10.1021/acs.macromol.2c00264.

(22) Surnar, B.; Jayakannan, M. Delivery under the Gastrointestinal Tract. *Biomacromolecules* **2013**, *14*, 4377–4387.

(23) Surnar, B.; Subash, P. P.; Jayakannan, M. Biodegradable Block Copolymer Scaffolds for Loading and Delivering Cisplatin Anticancer Drug. *Zeitschrift fur Anorg. und Allg. Chemie* **2014**, *640* (6), 1119–1126. https://doi.org/10.1002/zaac.201400030.

(24) Hu, R.; Yang, X.; Qin, A.; Tang, B. Z. AIE Polymers in Sensing, Imaging and Theranostic Applications. *Mater. Chem. Front.* **2021**, *5* (11), 4073–4088. https://doi.org/10.1039/d1qm00078k.

(25) Deshpande, N. U.; Virmani, M.; Jayakannan, M. An AIE-Driven Fluorescent Polysaccharide Polymersome as an Enzyme-Responsive FRET Nanoprobe to Study the Real-Time Delivery Aspects in Live Cells. *Polym. Chem.* **2021**, *12*

(10), 1549–1561. https://doi.org/10.1039/d0py01085e.

(26) Ghosh, R.; Jayakannan, M. Theranostic FRET Gate to Visualize and Quantify Bacterial Membrane Breaching. *Biomacromolecules* **2023**, *24* (2), 739–755. https://doi.org/10.1021/acs.biomac.2c01202.

(27) Liu, X.; Zeng, Y.; Liu, J.; Li, P.; Zhang, D.; Zhang, X.; Yu, T.; Chen, J.; Yang, G.; Li, Y. Highly Emissive Nanoparticles Based on AIE-Active Molecule and PAMAM Dendritic "Molecular Glue." *Langmuir* **2015**, *31* (15), 4386–4393. https://doi.org/10.1021/acs.langmuir.5b00155.